CHALMERS
UNIVERSITY OF TECHNOLOGY

Design of type IV compressed gas hydrogen tanks made of carbon fiber composites for sustainability and circularity

Master's thesis in Product Development

Philip Ngo
Antony Alfred Mohan Irudayaraj

Department of Technology Management and Economics

CHALMERS UNIVERSITY OF TECHNOLOGY
Gothenburg, Sweden 2024
www.chalmers.se

Master's thesis 2024

Design of type IV compressed gas hydrogen tanks made of carbon fiber composites for sustainability and circularity

PHILIP NGO
ANTONY ALFRED MOHAN IRUDAYARAJ

CHALMERS
UNIVERSITY OF TECHNOLOGY

Technology Management and Economics
Chalmers University of Technology
Gothenburg, Sweden 2024

Design of type IV compressed gas hydrogen tanks made of carbon fiber composite for sustainability and circularity

Supervisor: Frida Hermansson, IVL
Supervisor: Monica Johansson, Volvo GTT
Examiner: Magalena Svanström, Technology Management and Economics

Master's Thesis 2024
Department of Technology Management and Economics
Chalmers University of Technology
SE-412 96 Gothenburg
Telephone +46 31 772 1000

Cover: Visualization of hydrogen fuel tank constructed in CAD.

Typeset in LaTeX
Printed by Chalmers Reproservice
Gothenburg, Sweden 2024

Design of type IV compressed gas hydrogen tanks made of carbon fiber composite for sustainability and circularity
Philip Ngo
Antony Alfred Mohan Irudayaraj
Department of Technology Management and Economics
Chalmers University of Technology

Abstract

The transition to sustainable energy sources has highlighted the potential of fuel cell electric vehicles and the use of hydrogen as a clean fuel alternative. Central to the deployment of hydrogen-powered vehicles is the development of efficient and reliable hydrogen storage solutions. This project focuses on the design of Type IV compressed gas hydrogen tanks made of composite materials, aiming to enhance sustainability and circularity. The Type IV tanks being made of carbon fiber as the main component constitutes a high percentage of carbon dioxide footprint in the vehicle, since it is high energy intensive to produce and traditionally use petroleum based products as a primary raw material. Reducing the carbon dioxide footprint from this product would have a huge impact in the whole vehicle. This study investigates approaches to reduce the usage of carbon fiber and virgin carbon fiber in hydrogen tanks. The methods such as mass optimization, patch reinforcement, and recycled carbon fiber substitution were explored by testing it in a virtual model of the tank using Abaqus software. The results demonstrate that these approaches can significantly reduce the amount of carbon fiber required, potentially leading to a substantial decrease in the overall carbon footprint of fuel cell electric vehicles. Furthermore, the study explores the impact of these approaches that reduces the carbon fiber usage influence the factors like material usage and stress distribution within the tank.

Keywords: Optimisation, recycled carbon fiber, patch reinforcement, doily, Sustainable design, carbon fiber, FEM.

Acknowledgements

We would like to express our sincere gratitude to several individuals who significantly contributed to this project.
Monica Johansson, our supervisor at Volvo Trucks Technology, provided invaluable knowledge, guidance, and support throughout the entire project. Her expertise was instrumental in our success.
Anton Hagby not only shared his knowledge of Abaqus modeling but also offered a wealth of insights and tips specifically related to hydrogen tanks and composite material design. His contributions were exceptional.
We are grateful to our examiner, **Magdalena Svanström**, and our supervisor at Chalmers, **Frida Hermansson**, for their additional guidance on subject of Carbon fiber, LCA, sustainable design and for continuously emphasizing the importance of learning. Their dedication to our education is truly appreciated.
Our thanks extend to **Volvo Trucks Technology** for providing us with workspace, computers, and the resources necessary to complete this project. Finally, a special thanks goes out to all our colleagues at Volvo Trucks Technology. Their warm welcome and willingness to include us in their group fostered a friendly and supportive work environment, which we greatly appreciate.

Authors, Gothenburg, June 2024

List of Acronyms

Below is the list of acronyms that have been used throughout this thesis listed in alphabetical order:

BEV	Battery Electric Vehicle
BOM	Bill of Material
CAD	Computer Aided Design
CAE	Computer Aided Engineering
CE	Circular Economy
CF	Carbon fiber
CRFP	Carbon fiber reinforced polymer
DFMEA	Design Failure Mode Effect Analysis
DfS	Design for Sustainability
DP	Design pressure
DOE	Design of experiments
FCEV	Fuel cell electric vehicle
FEA	Finite Element Analysis
FOS	Factor of safety
LCA	Life cycle assessment
vCF	Virgin Carbon fiber
rCF	Recycled Carbon fiber
RPN	Risk Priority Number

Contents

1
Introduction

For decades, human mobility and economic growth have been powered by the internal combustion engine. However, many of the vehicles that connect and power human prosperity are among the largest contributors to environmental challenges such as including greenhouse gas emissions.With advancements in technology, communication, and trade, the world has become more interconnected and the population reaching 8 billion (Meardon, 2018) the demand for transportation has increased. Unfortunately the majority of the vehicles are ICE vehicles fueled by fossil fuels and that has led to a huge increase in greenhouse gas emissions. Land, air and sea transportation accounts for almost a third of the world's carbon dioxide emissions (Teter, 2023).

Volvo Trucks Technology's goals and commitment aligns with the ambitions and climate change goals set forth by the Paris Agreement energy (Johansson, Volvo Principal Energy and Fuel Analyst). Looking at the lifecycle of Volvos vehicles, the primary contributor to carbon emission occur during the use phase. This insight has led to prioritizing developing solutions that reduce emissions from transportation. Among such solutions is the Fuel Cell Electric Vehicle (FCEV), which is primarily meant for long distance operations. The FCEVs therefore complement BEV as they offer an alternative to BEV in areas where charging infrastructure is limited. Furthermore, the fact that FCEV has the ability to be refueled with hydrogen quickly makes them a compelling option. However, the use of FCEVs are faced with a number of challenges, among them are the need to store hydrogen at very high pressure. This requirement creates the need to use lightweight and strong CF tanks that can support high pressure while remaining light in weight.

A critical sustainability concern arises with the production of CF composites for hydrogen tanks. Studies shown by Weiszflo and Abbas (2022) claim that very energy-intensive processes for CF composites may offset the potential benefit of their lighter weight. Therefore, recycling appears as a promising avenue to significantly reduce the environmental impact of CF composites. But for recycling to be truly viable, the recovered materials from the tank need practical applications in new products or materials. This would create a more sustainable resource management system. Another option to reduce the environmental impact can be to explore different manufacturing processes and product design optimization. Second-life applications for CF is another area of research which can be pursued. This is because the current end-of-life treatment for CF in type IV hydrogen tanks is to simply disassemble them and treat them as scrap (Benitez and et al., 2021). Instead, this approach of disposing of them the end of their life cycle, alternative uses or application are

desired for the CF. Andrew Wright (2022) suggests the case of considering re-use in other applications, such as uses in the automotive industry or other sectors requiring lightweight and durable materials. Another approach is to refurbish or remanufacture the CF composite components. This involves detangling, milling, cutting and preparing the CFs to give them a new life or extending their lifespan and adapting them for diverse contexts (Tyson, 2020). This strategy offers the most utility to materials by discovering new applications for materials. The other concept being explored is upcycling. Upcycling involves CF components being transformed to higher value products or materials through design methods. This approach promises sustainability and resource efficiency through material reduction, entailing environmental impacts associated both with CF production and disposal. The actual effects of upcycling on the environmental impact and performance for hydrogen tanks are however under investigation.

1.1 Aim

This thesis investigates and optimizes the design of a hydrogen fuel tank for Volvo Trucks Technology. The focus will be on sustainability and circular economy. This will be done by identifying the key parameters that affects the environmental impact and finding ways to reduce them.

1.2 Research questions

The objective is to design a Type IV tank made of CF by utilizing DfS strategies and CE. To solve this objective, the following research questions need to be answered.

- How does the variation in carbon fiber composite mass and design impact the tank's stress, strain and mass?
- What are the most effective strategies to reduce the mass of virgin carbon fibers in the tank?
- How do different tank manufacturing methods impact the mass of carbon fiber in the tank?
- Can recycled carbon fibers be used in the tank design while meeting the performance and factor of safety for a hydrogen storage?

2
Theory

The chapter represents a theoretical framework of the design of a hydrogen fuel tank with all the possibilities and methods for the reduction of environmental impact. This begins with the exploration of hydrogen as an increasingly used fuel source. Following this, the solutions for storing hydrogen, the types of tanks and winding patterns and techniques used. After this, the chapter closes with an explanation of CE and sustainable design. This theoretical background will aid the reader with the necessary knowledge to approach the design challenge with a focus on responsibility towards the environment.

2.1 Hydrogen in transportation sector

As the urgency to combat climate change intensifies, the transportation sector needs a cleaner energy source. Here, hydrogen gas (H_2) emerges as a promising alternative (Gencer, 2021). Unlike fossil fuels that emit carbon dioxide and are one of the main driver of climate change, hydrogen fuel cells can have close to zero greenhouse emissions if carbon neutral hydrogen is used. This significantly reduces a vehicle's environmental impact by mitigating climate change. Moreover, dependence on hydrogen gas reduces the demand for fossil fuels and provides resource conservation. But while challenges remain in terms of production cost and the development of infrastructure, hydrogen fuel has huge potential for a greener future (Gencer, 2021). On the contrary, hydrogen does not occur in an easily usable form on earth. To run these vehicles with it as fuel, it has to be produced by extracting it from other sources. There are mainly three methods of production:

Thermal Process: This is the most common method used for large-scale hydrogen production and is referred to as steam reforming or grey hydrogen (Energy.Gov, n.d.-a). This process involves utilizing the high-temperature reaction of steam (H_2O) with natural gas (CH_4) in the presence of a catalyst. The result of this reaction is the production of both hydrogen and carbon dioxide. While this process still results in greenhouse gases, it reduces half the emissions released into the atmosphere during production, transportation and storage compared to today's fossil fuel powered vehicles (Energy.Gov, n.d.-c).

Electrolysis: The process electrolysis which is also known as green hydrogen offers a cleaner alternative by splitting water molecules (H_2O) into hydrogen and oxygen using electricity instead of fossil fuels (Energy.Gov, n.d.-a). This process requires less energy compared to that in steam reforming, but this whole process still remains energy-intensive. The impact on the climate due to electrolysis heavily depends upon

where its electricity originated from. If the electricity comes from such renewable sources as solar or wind power, then this will be a clean and sustainable method of production of hydrogen (Energy.Gov, n.d.-b).

Natural hydrogen extraction: White hydrogen or gold hydrogen exists naturally underground and can be extracted in two ways (Le, 2024). The first process involves drilling deep wells that reach to such geological layers where white hydrogen is trapped. Another methodology focuses on the separation techniques of white hydrogen from water sources. White hydrogen identifies a very promising concept with no carbon dioxide, but it is still under development. This is because its extraction in large volumes with low environmental impact is yet to be achieved (Vujasin, 2023).

2.2 Hydrogen Storage

Hydrogen storage systems are special containers engineered to hold hydrogen in its gaseous or liquid form. It is also possible to hold in the solid form with chemically bound state within metal hydrides, but this is not as efficient. The tanks therefore play a vital role in the use of hydrogen as a clean fuel. FCEVs use hydrogen to produce electricity through an electrochemical process. The hydrogen stored in the tank flows into the fuel cell and reacts with oxygen from the air to yield electricity and water vapor. This electricity drives the vehicle's electric motor, resulting in zero tailpipe emissions. Therefore, hydrogen fuel tank technology offers immense potential for a sustainable future for transportation. However, one of the critical challenges is how to safely and efficiently store hydrogen gas in containment vessels subjected to very high pressures (Energy.Gov, n.d.-d). Carbon fiber in that respect becomes a promising material as a reinforcement in making hydrogen storage solutions robust and lightweight. Carbon fiber composites are materials that bring out the best of two worlds: incredibly strong and stiff, thin strands of carbon fibers and a surrounding polymer resin to hold them together (DragonPlate, n.d.). Those properties translate into ideal properties for hydrogen storage tanks. The exceptional strength-to-weight ratio allows for robust tanks that can withstand high pressures yet still being lightweight. There exists four types of hydrogen tanks which are classified based on their construction and pressure rating (Hyfindr, 2024):

- **Type I**: These are made from metal cylinders for low-pressure storage. However Type I tanks have a limited usage in FCEVs since their capacity is rather low (Barthelemy, 2017).
- **Type II**: These are made from high strength steel with aluminum or CRFP wrapped around the cylindrical part. Type II tanks can handle higher pressures and have some application in industrial uses.
- **Type III**: These are made with an aluminum liner that is wrapped in carbon fiber to give a good balance of strength to weight ratio. They are used to store compressed hydrogen storage in some FCEVs, this type of tank does not have a separate boss component but the inner line and the boss is a single unit.
- **Type IV**: These are made from a polymer inner liner wrapped with a high strength carbon fiber composite material, these tanks are the most common

type used in FCEVs. This tank will be the focus of the study and its main components are the boss structure, inner liner and outer carbon fiber layer composite (see Figure 2.1)

Type II, III, and Type IV tanks utilize carbon fiber reinforcement in the windings. These are carefully wrapped around the plastic liner in specific patterns (hoop, helical, dome) to achieve the required strength and pressure resistance.

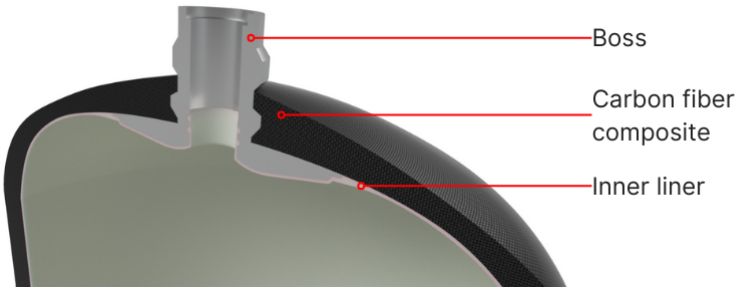

Figure 2.1: Illustration of type IV tank and main components

2.2.1 Winding pattern

The purpose of winding patterns is that it provides an even distribution of pressure load across the tank withstanding high pressures of hydrogen storage. The Figure 2.2 below shows the three most common winding patterns (JEC, 2022). These patterns are normally used in a combination of hoop, helical, and dome reinforcment to arive at the best possible strength and pressure resistance across the entire tank. The ratio and the placing of each pattern will depend upon the desired tank design, pressure rating, and weight characteristics. For example, if a tank needs to have high longitudinal stress for a specific application, it might have a higher percentage of helical windings compared to a design focused on withstanding internal pressure.

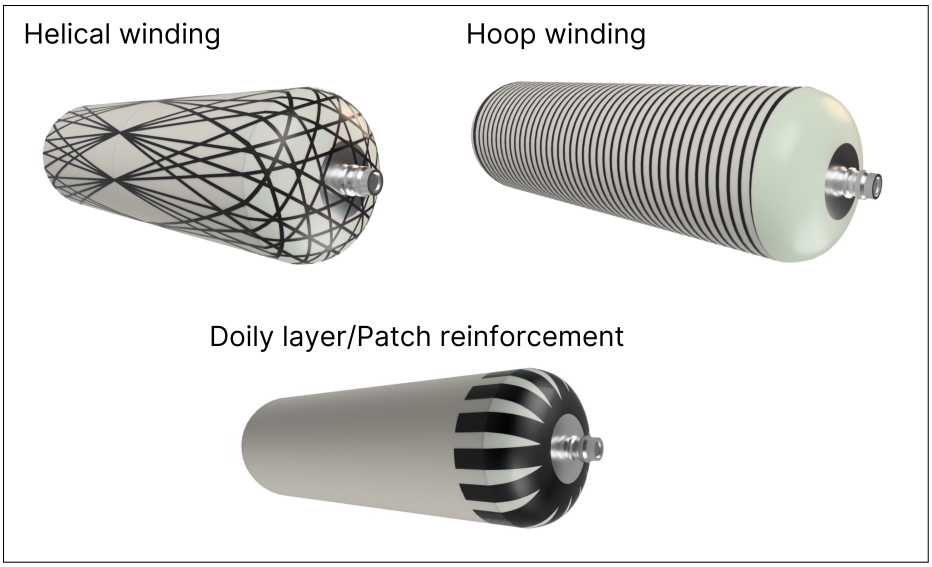

Figure 2.2: Different winding patterns in pressure vessels

- **Hoop Winding (Circumferential)**: In hoop winding, the carbon fibers are oriented circumferential around the cylindrical body of the tank. The angle of hoop winding is therefore close to 90 degrees, with the fiber path nearly perpendicular to the longitudinal axis of the tank. This pattern is excellent for strengthening the tank against pressure trying to burst it open like a balloon. This pattern provides most of the resistance to hoop stress, as well as to internal stress and circumferential tension in the tank wall.
- **Helical Winding**: Helical winding consists of wrapping carbon fibers around the tank in a helical or spiral pattern. These fibers tend to be at an inclined angle which usually has the span from 10° to 80° with respect to the longitudinal axis of the tank. This winding creates the pattern which can be seen in the Figure 2.2 above. The angle in helical winding is critical to ensure that there is a proper balance between contribution to both the hoop strength and the ability to take longitudinal stress—splitting the tank lengthwise. The specific helical angle chosen for a tank design significantly impacts this balance and is divided between high and low helical angles.

  Low Helical Angle (10° - 45°): With tanks experiencing significant longitudinal stress there is a need for low helical angles. This is due to fibers oriented closer to the tank's long axis, the design offers superior longitudinal strength and also reasonable hoop strength at the same time. However, low helical angle results in a slightly heavier design in the construction of the hydrogen tank.

  High Helical Angle (45° - 80°): By aligning the fibers more closely with the outward pressure, a high helical angle offers increased efficiency for pressurized gas containment. That means high helical angles achieves the required hoop strength at a lower material usage, making the tank lighter. But, the longitudinal strength provided by it is less in comparison to that offered by a low helical angle. For high-pressure tanks or those requiring significant longitudinal strength, a high helical angle might necessitate additional reinforcement strategies.
- **Dome Reinforcement**: Dome reinforcement which is also referred to as doilies or patch reinforcement focuses on strengthening the weaker parts of the tank by adding material. This would typically be the case for the dome-shaped ends of the tank. In dome reinforcement the fibers are placed over the dome section of the tank in a precise way. The purpose of these fiber is to distribute the pressure evenly and retain some stress from the helical layers. These dome ends are particularly prone to pressure due to their curved shape, and against such pressure dome reinforcement provides crucial reinforcement.

2.2.2 Filament winding

Filament winding is a well-established technique for manufacturing of composite parts, such as high-pressure tanks for hydrogen storage. The method offers several advantages, including high strength-to-weight ratios, excellent corrosion resistance, and design flexibility. The filament winding process presented below is an overview of the key steps involved in the filament winding process of carbon fiber hydrogen

tanks (Azeem and et al, 2022):

- **Mandrel Preparation**: First, a rigid mandrel replicating the desired tank geometry is created. The mandrel, typically cylindrical for hydrogen storage, can be made from metal or composite materials.
- **Resin Application Techniques**: There are two primary approaches for resin application during filament winding:
  - **Wet Winding**: This is essentially a process where continuous fibers are pulled through a resin bath immediately before laying them up on the rotating mandrel. Wet winding offers a high degree of efficiency and cost-effectiveness, making it well-suited for high-volume production (Addcomposites, 2022).
  - **Dry Winding**: In contrast to wet winding, dry winding primarily make use of prepreg carbon fiber in which the fibers have already been pre-impregnated with resin before being wound onto a mandrel. This provides much more control over the final fiber-to-resin ratio giving possibly better consistency of product but at a higher cost.
- **Fiber Path**: The fibers follows a specific path, this is often called a geodesic path which focus on reinforcement around the tank's circumference to handle internal pressure.
- **Resin Curing**: The last step of filament winding is resin curing. This is where the resin undergoes curing which results in matrix solidification and rigidity. The method of cure would be based on the particular resin system adopted and can range from heating, pressure, or a combination.

Fiber Reinforcement: This is a critical filament winding material. Prepreg is carbon fibers pre-impregnated with a thermosetting resin system, essentially pre-coated with resin. Towpreg is a specifc type of prepreg where the fibers are bundled into "tows" before being impregnated with resin. Prepreg offers different advantages such consistent resin content, reduced processing time and improved quality (Addcomposites, 2022).

2.3 Circular Economy

The interest in CE has grown as a response to the increasing concerns about resource depletion and waste generation, having been directly linked to sustainable development (Böckin et al., 2020). As a result of this, Volvo Trucks Technology is actively integrating CE principles and the nine R-strategies into their products (Trucks, 2024). But despite the rapid rise to popularity, there is currently no universally agreed-upon definition of the CE. This is due to the broad scope of the CE and that the definition of CE consists of a wide range of practices and strategies, along with a variety of how it can be implemented. This very broadness makes it challenging to capture all its aspects in a universally and concise definition. Furthermore, CE is a relatively new concept and is continuously changing as new technologies and approaches is discovered. This constant development makes it hard to pin down a single definition which remains relevant over time (Billing, 2021). Nevertheless the CE is still a model that moves away from the traditional "take-make-dispose" approach towards resource consumption. Resources in this model are seen as main-

taining their value and not allowed to become waste. This is achieved by keeping products and materials circulating for as long as possible while generating less waste to promote regeneration in nature. Such circular strategies are based on reuse and repurposing which forms the backbone of CE. As highlighted by the Ellen MacArthur (Foundation, 2021), these strategies are driven by three underlying design principles:

- Eliminate waste and pollution
- Circulate products and materials (at their highest value)
- Regenerate nature

2.4 Sustainable Design

Sustainable design is a concept that emphasizes creating products, services and systems that minimize environmental impacts throughout their entire lifecycle (Mouëllic et al., 2023). DfS strategies are particularly relevant for systems like hydrogen fuel tanks. This is because these strategies directly address environmental concerns by tackling climate change and conserving resources through practices that reduce resource depletion, pollution and waste. Sustainable design goes beyond just environmental benefits. It fosters a CE by encouraging the design of products that are easier to disassemble, reuse and recycle. These systems minimize waste and ensure resources are available for future generations. Six different DfS strategies exist throughout the product lifecycle, which includes:

- Dematerialization
- Material Selection
- Green Supply Chain
- Longevity and Effective Usage
- Product Efficiency
- Circularity

3
Methodology

This chapter outlines the methodology adopted for developing and evaluating a sustainable hydrogen fuel tank, which can be seen in Figure 3.1. The methodology draws inspiration from the development process proposed (Johansson et al., 2019), but are further elaborated upon in the following sections. This comprehensive approach gave an in-depth understanding of the state of knowledge in hydrogen fuel tank design with a particular regard to DfS and CE principles. Following this, there was a need to define a detailed requirement specification that would outline the product functionalities, performance targets and constraints. This documentation addressed the creation of a BOM with all the components to be used and a DFMEA detailing possible failure modes and how they would be addressed. In the design generation process a computational and CAD software were used. The design process also adopted an iterative process, which involved revisiting previous stages and testing result to continuously refine the design. Finally, the design was evaluated against the requirements by ensuring it meet the requirements and performed as intended.

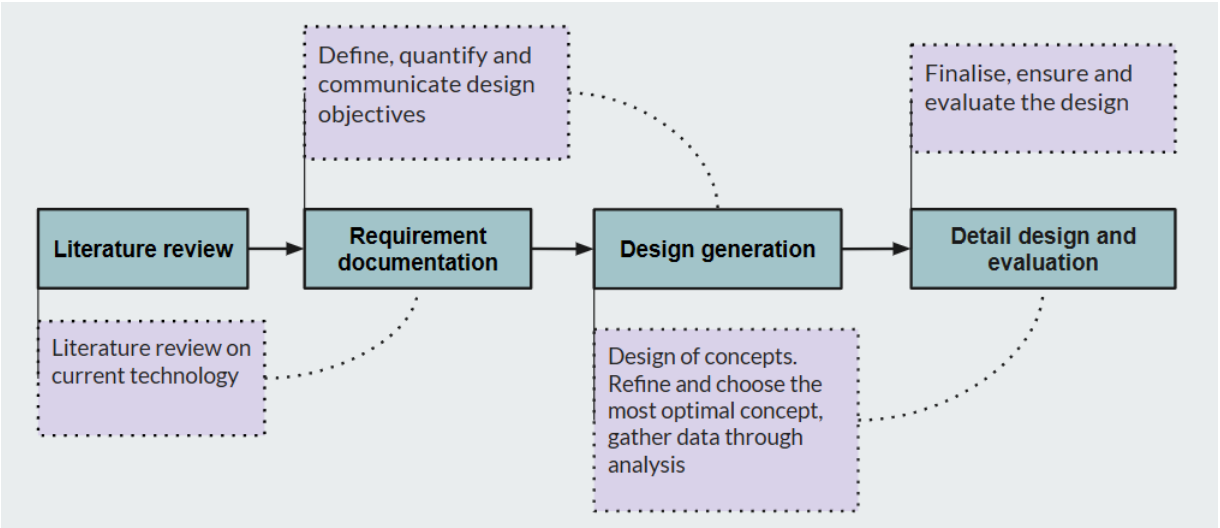

Figure 3.1: Hydrogen Fuel Tank Design Methodology

3.1 Literature Review

A comprehensive literature review was made to inform the research on hydrogen fuel tank design. The review was primarily conducted on the period from January to February 2024, but additional sources from throughout the project timeframe were

also included. This literature review was based on the principles of the DFS and CE frameworks in the process of informing the research on hydrogen fuel tank design. Specifically, it focused on understanding the current state-of-the-art, identifying potential future improvements and discovering sustainable design practices.

- **Gather relevant knowledge** was the first step in the literature review which involved academic research. This was conducted through platforms like Google Scholar and ScienceDirect along with patent research which provided an in-depth understanding of the hydrogen fuel tank. Research was carried out to inform and identify potential gaps in knowledge, particularly within the framework of DfS and CE (see tbl. 3.1). This included understanding established DfS principles and exploring successful CE implementation in similar product development processes and tank technology. Analyzing existing hydrogen fuel tank products provided insights into the current state-of-the-art. Finally, any further resources that could usefully contribute to the understanding of the current practice and possible future developments were considered.

Table 3.1: Topics for literature study

Category	Topic
Tank Design & Technology	Manufacturing/production process of hydrogen tanks
	Comparison of different pressure tanks
	Design requirements of hydrogen fuel tanks
	Future advancements in hydrogen fuel tanks
Sustainability & Circularity	Sustainable design techniques
	Circularity methods
	Methods to lower carbon footprint
End-of-Life Management	End of life of hydrogen fuel tanks

- **Key experts** in the field with knowledge of DfS and CE principles as applied to hydrogen fuel tank design were identified and interviewed. The experts were chosen based on their understanding on different disciplines such as material, structure and manufacturing of the hydrogen tank.
- **Focused interview questions** were developed that would help in understanding the research questions in greater depth. Guided interviews with Volvo Trucks Technology engineers and other experts, such as hydrogen fuel tank designers, CAD and CAE engineers were created. Interviews provided information on specific technical and operational requirements for hydrogen fuel tank design and how CAE tools are used within the design process. Additionally, views and concerns from the stakeholder regarding the implementation

of hydrogen fuel tanks were discussed during the interviews. The interviews included discussions about the potential for mass reduction and implementation of rCF for the hydrogen fuel tank, exploring how this could contribute to Volvo's long-term goals for sustainable transportation.

3.2 Requirement Documentation

Following the literature review, a comprehensive requirement specification was developed for the hydrogen fuel tank design. This documentation was to clearly document the criteria that guide the design process. These criteria served as a benchmark for evaluating and selecting the most suitable design concepts, see Appendix A.1 for more information tank and section **4.1 Design Parameters**. For the requirement specification, information was gathered through a comprehensive literature review and interviews with engineers from Volvo Trucks Technology and other relevant experts. Structured format was used in documenting the requirement specification, which captured the following key elements for the specification:

- **Functional and non-functional requirements**: In this category, the requirements specified were specific and measurable, such as DP and dimensions.
- **Target values and requirements/wishes**: For every single requirement, specific target values as well as acceptable ranges were laid down. Desirable attributes were also identified and documented but this was not mandatory.
- **Weighting**: Every requirement was rated against a relative weighting or importance. This allowed a prioritization between requirements during the design process and allowed for a trade-off analysis.
- **Verification methods**: Different methods were established to verify that the final design meets the specified requirements, such as simulations, testing, and expert review.
- **Stakeholder**: Identified key stakeholders and incorporated their input into the specificatios that addressed their specific needs and priorities.

3.2.1 Bill of material

A BOM was utilized to define the necessary components for the construction of the hydrogen fuel tank(Grant, 2023). This BOM documented:

- A **comprehensive list** of all components required for the tank assembly.
- **Descriptions** of each component, including its function and purpose.
- **Material specifications** for each component, ensuring compatibility and appropriate properties for hydrogen storage.
- **Quantities** of each component needed for assembly.

By detailing these elements, the BOM offered several benefits for the study and further design generation. The BOM provided detailed information about all the components and materials used, which instituted full understanding of what makes the tank's composition. (see Appendix A.2 for details). This information eased decision-making in further design process regarding design choices, material selection, and overall functionality of the finalized tank. Furthermore, the BOM enabled

design optimization. With a clear understanding of the details and interactions of individual components, factors related to the weight of the tank and efficiency and performance could be considered in optimizing a design.

3.2.2 Design Failure Mode and Effect Analysis

DFMEA was carried out to identify and reduce potential failure modes in the hydrogen fuel tank design (Christiansen, 2024). This systematic approach played a crucial role to analyze the interaction of various components and materials in the previously designed tank. While analyzing the interactions of materials and the components, it identified the potential consequences that lead to design flaws. This analysis enabled informed decisions regarding material selection and component integration, ultimately leading to a more precise and robust final design for the hydrogen fuel tank(see Appendix A.1 for details). The steps conducted for the DFMEA are shown below in the list:

1. **Design Review**: The process began by thoroughly examination of the design specifications and functionalities of the hydrogen fuel tank. This review considered the BOM and requirement specifications to ensure a clear understanding of the entire tank system.
2. **Failure Modes**: Following the review, a brainstorming session identified all possible ways the tank design could fail to meet its intended function.
3. **Listing Failure Effects**: The likely consequences and effects that could result from each of the identified failure modes were recorded against their respective listing on the tank.
4. **Severity Ranking**: A numerical ranking on a scale from 1 to 10 was assigned to each failure mode. This ranking reflected the severity of the consequences that could have occurred due to the failure mode and its effects. Higher numbers represented greater severity.
5. **Occurrence Ranking**: The likelihood of each failure mode and its effects occurring were estimated based on a literature review, interviews with relevant personnel and judgment. A numerical ranking system was again used to represent the probability of occurrence, higher numbers indicating a greater likelihood of the failure happening.
6. **Detection Ranking**: The final ranking system evaluated the effectiveness of the implemented controls in detecting these failures modes before they occurred. Rankings were based on how likely these controls would be to catch the issue. Higher numbers indicated a lower likelihood of being detected by the controls.
7. **RPN Calculation**: The RPN was calculated for each failure mode by multiplying the number of the severity, occurrence and detection rankings. This score provided a indication of the overall risk associated with each failure mode, helping to prioritize which ones required the most attention for mitigation strategies.

3.3 Design Methodology

Following the establishment of requirements in the previous section, the focus shifted to generating a diverse set of potential design concepts for the hydrogen fuel tank. This stage aimed to explore a wide range of possibilities to ensure an optimal solution was identified. The design methodology used is illustrated below in Figure 3.2. This section will explain the underlying theory and the different stages involved in this methodology. For a detailed explanation of how the methodology was applied, refer to **Chapter 4**. The design process for the hydrogen fuel tank can be broken down into four key phases which will be explained in detail below.

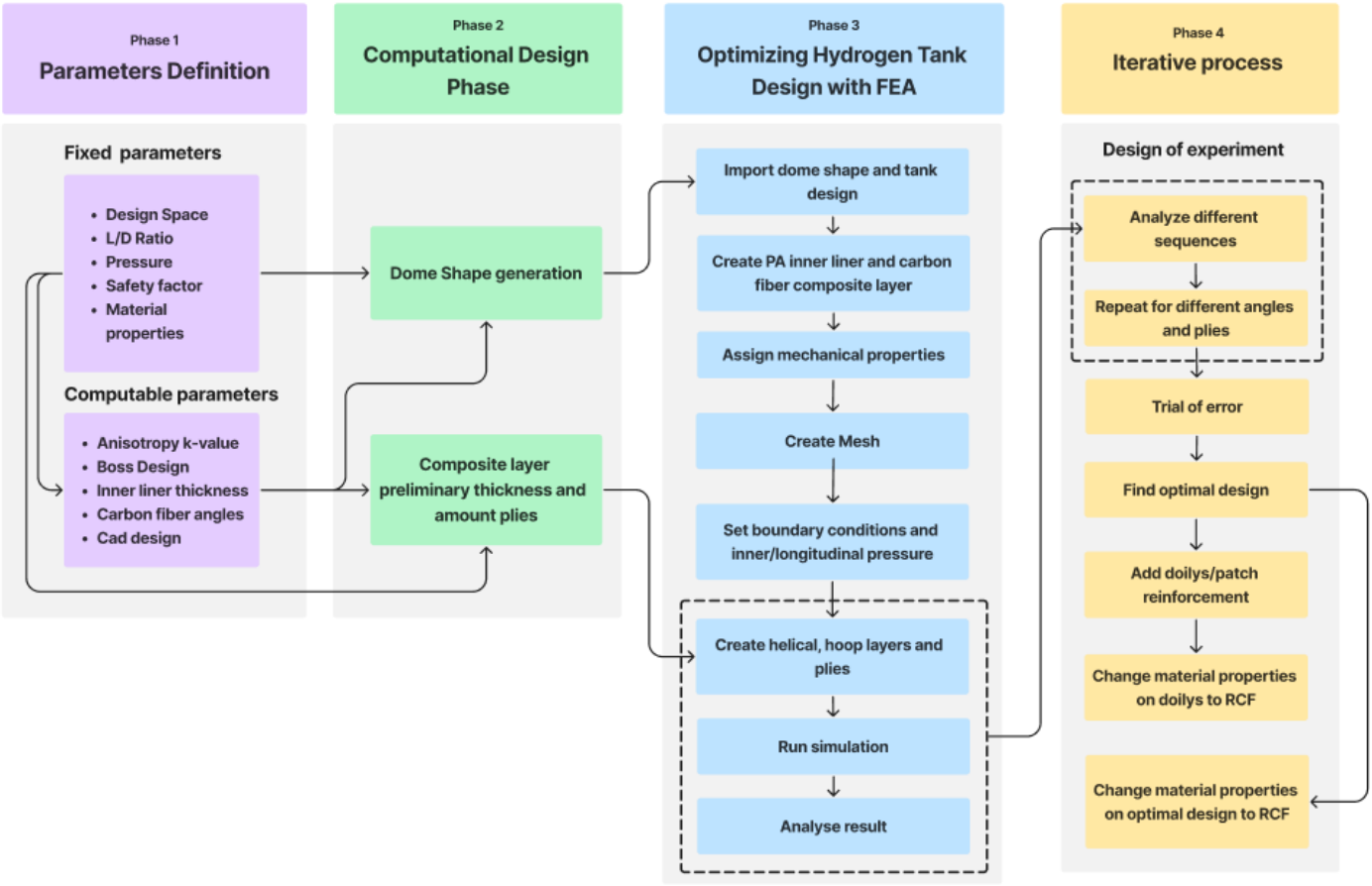

Figure 3.2: Design Method for hydrogen tank

1. **Parameter Definition** The initial phase of the hydrogen fuel tank design process began with defining key parameters. These parameters were divided into two groups:
   - **Fixed parameters**: These are fixed values that are set by either Volvo Trucks Technology, collaborating suppliers, or identified from literature review.
   - **Computable parameters**: These parameters require calculation through equations, formulas to be determined or were necessary parameters for dome shape generation and thickness calculation.

2. **Computational Design Phase** This phase involved the use of a computational tool called Python. This was done to determine the shape of the dome, the thickness of the preliminary carbon fiber layer and the number of plies required for the FEA phase
    - **Dome shape generation**: For the dome shape generation understanding the mechanical property of the material was crucial. One key concept for CF and the dome shape was orthotropy. This term means that the material's stiffness varies depending on the direction of applied stress (Sazedul Islam and et al, 2022). Wood is a common example of an orthotropy material because it is stiffer when bent along the fibers compared to when it is bent across the fibers. This change in stiffness within a material is measured using a value called the k-value. A k-value of 1 signifies a uniform material with equal stiffness in all directions, known as isentropic. In contrast, a k-value less than 1 indicates an orthotropic material where stiffness is higher along the fiber direction and relatively low across the fibers. The understanding of k-value is important while designing such structures that make use of orthotropy, for example CF. By taking into account the variable stiffness of the material, an optimal design for strength and lightweight is also achievable in a lightweight tank. This optimization process involved generating the dome shape which was a key component influencing the tank's structural performance. The primary objective was to ensure that the resulting dome could safely handle the loads that would be on the tank.
    - **Preliminary thickness calculation**: During the design phase, a crucial step involved calculating a preliminary thickness for the CF layers in the dome. This preliminary thickness was done to achieve the desired balance between the tanks strength and weight. A technique called netting analysis was employed. This is a simplified method which considers the mechanical properties of the CF stiffness and stress to estimate the thickness required for the dome to withstand pressure loads. Although not as advanced as the FEA used later, netting analysis gave a fast and effective way to determine a starting point. This calculated thickness served as an initial estimate for the number of ply layers needed in the design. A thicker layer is stronger but heavier, so optimization is required to arrive at the best balance between these two critical factors.
3. **Hydrogen tank design using Finite Element Analysis**: This is a crucial step which allowed for a more refined approach in optimizing the performance and reducing the mass of CF in the tank. The previously generated dome shape, preliminary CF layer thickness and other relevant parameters were incorporated into the FEA model. Following this, Abaqus software was then used to find the optimal CF angle sequence and thickness (Systèms, 2024). The aim of the optimization was to find a design with minimized weight of CF, but still ensuring the tank could withstand the anticipated stresses and strains during operation.
4. **Iterative process**: The iterative phase focused on achieving a sequence of carbon fiber plies with low stress and strain for the final hydrogen fuel tank.

This phase also aimed to provide a better understanding of how the variation in carbon fiber mass and design impact the tank. DOE played a very crucial role in this phase. This systematic method analyzed the relationships between various factors (layer sequences, angles, and ply count) and their output(impact on achieving low stress and strain). Through DOE testing, different combinations of these factors were evaluated to identify the design that minimized mass while meeting these performance requirements. An iterative trial-and-error process followed, which further refined the design for low stress and strain by analyzing the DOE results and strategically combining different layer sequences, angles, and ply counts. Finally, based on the optimized design, tank construction incorporating different manufacturing methods, such such as patch reinforcement(doilies), recycled CF and designs with lower safety factor.

3.4 Methods of Carbon fiber reduction and optimization

Ply Angle: Modifying the ply angles and their sequence in CF tanks are the most common process for reducing CF mass in hydrogen tanks. This is due to the approach facilitates both an even stress distribution and a more efficient use of materials, ultimately contributing to a DfS concept.
Patch reinforcement: Patch reinforcement is a new manufacturing method which is also known as doily layers. This method is highly effective for reducing CF mass in tanks by strategically apply patches of CF to sensitive areas of the tank such as the dome (similar to the 90-degree doily layer shown in the bottom image of Figure 2.2.). By applying these patches, the amount of CF layers can be reduced in other portions of the tank and reduce the overall CF mass in the tank.
Material substitution: As a DfS strategy, this alternative method explores substitute materials with tensile strength comparable to CF. However, there is a lack of materials that matches carbon fiber's weight-to-strength ratio. Although glass fiber, basalt fibers, kevlar and some natural fibers (as cited in Siddiqui and et al, 2023) are potential options, studies have shown that glass fiber can be environmentally detrimental compared to CF (Hermansson et al., 2022). Basalt fiber shows promise as a substitute material because it can be melted and remolded. However, combining basalt fiber with CF could introduce complications. The mixture of two different fibers in the resin might hinder the recyclability of the CF in the tank. This study is dedicated to exploring the use of rCF as a substitute, necessitating additional research to evaluate this potential issue.

3.5 Evaluating Designs Through Life Cycle Inventory and Assessment

The designs will be generated with the data from the research done in the paper (Kaliswal, 2024) and based on the recycling options and the material properties

suggested, the designs are created and evaluated in ABAQUS software. With the evaluated designs, a life cycle inventory will be created which can be used for assessing the design based on the climate change and carbon footprint. This assessment will provide a deeper understanding on how good the designs are. In this inventory, the mass of every component is listed, such as the liner, resin, virgin carbon fiber and recycled carbon used in a design. Additionally the energy required to produced the design with patch reinforcement technique.

Robotic arm energy calculation: The energy consumption is calculated for LCA study that could be done to compare between different designs. The energy consumption values utilized in this analysis are based on the findings presented in the paper by Liu, 2018. Liu's research investigated the energy consumption of a robot performing a pick-and-place task. The specific task sequence involved the robot moving from point A to B. The total energy consumption for this ten-second sequence from point A to B was measured and used in this analysis. Here, it was considered a scenario in which a single patch of 68mm width would be used for this task. To cover the entire dome section, an estimated 30 strips were determined to be necessary. Based on the Abaqus design, each patch reinforcement required 18 plies. Consequently, a total of 540 individual strips would be required for one of the dome in the tank. The energy consumption for placing a single CF strip on the dome, from the analysis of the pick-and-place task, was estimated at 2852 J. Extrapolating this value to the entire dome, the total energy required to place all 540 strips would be approximately 1540080 J. Since the tank design utilizes two domes, the total consumed energy for the patch reinforcement on the two domes of each tank is approximately 3.08 MJ. The analysis also considered the energy consumption of the vacuum suction tool assumed to be necessary for holding the strips during placement. A 500-watt vacuum was chosen for this purpose. The estimated time required to complete the patch reinforcement task on a single tank, considering the number of strips and the assumed tool, was 11600 seconds. The total energy consumption of the vacuum suction tool during this process is approximately 5.8 MJ. Combining the estimated energy consumption for the strip placement (3.08 MJ) and the vacuum tool operation (5.8 MJ), the total energy required to complete patch reinforcement on a single tank is approximately 8.8 MJ. Rounding this value to account for potential variations, a total of 9 MJ of energy is estimated to be required for patch reinforcement in one tank. From the result comparison shown in Table (5.10), design 3 and design 5 has the least vCF utilised (with respect to FOS 2.25 designs) proving that this method uses less carbon fiber. To further evaluate this design on the LCA perspective, the energy used to produce it must be included in the study and this paper (Assessing recycling opportunities for hydrogen tanks made from carbon fibre composites, Kaliswal, 2024), an LCA (Life Cycle Assessment) is performed to highlight the carbon dioxide footprint.

With these data, life cycle assessment (LCA) is conducted in the research paper (Kaliswal, 2024) to compare the designs determining which design, recycling option, and manufacturing process could be suggested for future development at Volvo Trucks Technology.

3.6 Limitations

This section explains the scope of the current project and clarifies boundaries. While this project will focus on optimizing the hydrogen tank design, there are some things outside the scope of this project:

- Manufacturing and production: This project utilizes simulations or analyses to optimize the design of a physical prototype, but does not involve its physical creation.
- A LCA calculation to quantify the environmental impacts of the design was not conducted.
- The design aspects of liner thickness, liner material and boss configuration have not been addressed in this project as they fall outside the current scope.
- Limitations exist in the analysis software due to its student license, where only 1000 nodes can be used to generate a model which would give 80% accurate results. And the outer layers of the composite material vessel cannot be analyzed as it would not provide the stress results

4

Design generation of the tank model

This chapter details the application of the design generation method outlined in section **3.3** to develop designs for a 700 bar, Type IV hydrogen pressure vessel. The following sections will detail the implementation of this methodology's key phases for the specific case of the hydrogen tank. These phases include design parameter definition, computational design, and the iterative process using FEA.

4.1 Design parameters

As illustrated in Figure 3.2, several key parameters were identified to ensure the hydrogen tank's successful integration within the vehicle. These parameters were divided into fixed and computable parameters which are described below in section **4.1.1** and **4.1.2**.

4.1.1 Fixed parameters

- **Design space**: This design space refers to the available area within the vehicle designated for the tank placement. The available space for the tank is a key constraint. Based on the available space and the L/D ratio will be constrained and the max limit will be set.
- **L/D ratio**: This ratio describes the balance between the tank's length (L) and diameter (D). Considering the chosen design space, the L/D ratio is set at 3.1. This value is derived from the 660 millimeter diameter and 2100 millimeter length. One other reason for choosing this particular ratio is that a 2100 millimeter length was chosen to meet existing testing procedures, as a longer tank (2400 mm) would require more expensive testing.
- **Pressure and Safety factor**: These were important factors in ensuring design of a robust hydrogen tank. The pressure and safety factor directly influence the tank's ability to withstand pressure, maintain structural integrity and store hydrogen safely. The design aimed to withstand 700 bar of pressure, which served as a fixed parameter. A safety factor was added to provide an additional margin of safety beyond the design pressure. This accounted for the pressure at which the tank would burst. By design, hydrogen pressure vessels are constructed to withstand pressures significantly exceeding their normal operating pressure. The design targeted a FOS of 2.25 for the model ISO,

2018. This translates to a theoretical capability of enduring pressures 2.25 times greater than the designed operating pressure. During the simulation phase utilizing Abaqus software, a FOS 2.0 ISODIS, 2024 was considered to evaluate the performance.

- **Material properties**: The properties of the materials used for the tank construction were crucial for the performance and safety. In the Abaqus simulation, key properties like Young's modules and Poisson ratio were consideration.
- **Boss Design**: The existing boss strcture from the current design was be retained. This decision ensured efficient CF wrapping or windability and avoided unnecessary material adjustments. Also, since the boss itself is made from a different material stainless steel or aluminum, the boss structure does not impact CF usage.
- **Inner liner thickness**: The liner was set to 5 mm. This parameter is critical as the liner needs to be thick enough to prevent hydrogen leakage and ensure tank safety.

4.1.2 Computional parameters

- **Anisotropy k-value**: A k-value of 0.088 was chosen for dome generation (Landi and et al, 2020).
- **Carbon fiber layer**: The orientation of the CF layers significantly affected the tank's strength under pressure. Optimizing these angles can improve overall performance.
- **CAD Design**: This digital representation integrated all the fixed parameters, allowing for detailed analysis and optimization of the tank's design.

4.2 Computational design phase

A Python script was used to determine the dome's shape and calculate the initial thickness required for the CF layer. These values were necessary to be imported into Abaqus for further analysis.

4.2.1 Dome shape generation

The shape of the dome is determined by solving a set of mathematical equations which can be seen below. These equations derived from Landi(2020) consider the k-value (Eq 4.1) of the CF material. The k-value reflects its directional stiffness and it played a key role in shaping the dome for optimal performance. By solving these equations for various values, this resulted in a series of points that defined the dome's surface (Eq 4.2). This process was efficiently done by using Python software, see Appendix (**A.3**) for script and input parameters.

$$k = \frac{E_2(1+\nu_{21})}{E_1(1+\nu_{12})} \qquad \text{(Eq 4.1)}$$

$$Z'(Y) = \pm \left(\frac{Y(Y^2 + rY_{eq}^2)}{\sqrt{\left(\frac{k+Y^{eq}{}^2-1}{k+Y^2-1}\right)^{k+1} Y_{eq}^6(1+r)^2 - Y^2(Y^2+rY_{eq}^2)^2}} \right) \quad \text{(Eq 4.2)}$$

Considerations for the dome shape:

- **Boss Radius (R_b) and cylinder radius (R_c)**: This represents the radius of the dome's top portion and the radius of the cylindrical part of the tank.
- **Radial coordinate (Y)**: This parameter defines the radial distance from the center, calculated with ρ/R_b with respect to Rb (Y $\geq$ 1).
- **Ratio of cylinder radius to boss radius (Y_{eq})**: This value is calculated as R_c/R_b.
- **Pressure parameter (r)**: This parameter represents the ratio of axial load to pressure and cylinder radius squared ($F_a/(PR_c^2)$).
- **Axial coordinate (z)**: This parameter defines the distance along the vertical axis of the tank.
- **Young's Modulus (E)**: This parameter quantifies stiffness to deformation under stress.
- **Poisson's ratio (ν))**: Describes the material's ability to deform in one direction when stressed in another

The Figure 4.2 below shows how different k-value influences the dome shape. A higher k-value (closer to 1) indicates a more isotropic material with less variation in stiffness across directions. This might result in a dome shape that is more rounded. In contrast, a lower k-value (0.088 for T700S CF) signifies a more orthotropic material with significant stiffness variation. This could lead to a dome with a slightly flatter profile or a more elongated shape to optimize strength in specific directions which can be seen in Figure 4.2. This picture illustrates the dome shape generated for T700S CF with the k-value 0.088 indicated in a red curve. The red curve is the shape of the dome with reference to the figure shown4.1 that is a quarter of the tank model.

4.2.2 Preliminary thickness

Drawing upon established equations, the thickness of the helical layer, denoted as t_∞ and hoop layer denoted as t_{90} can be determined using the following equations (Eq 4.3) and (Eq 4.4). This was efficiently handled using Python software by just input the values see Appendix(**A.1**) for python code and input parameters.

- P represents the burst pressure the tank is designed to withstand.
- R signifies the radius of the tank.
- $\sigma_{f,90}$ and $\sigma_{f,90}$ are the design allowable stresses of fibers in the hoop layer and in helical layer.

$$t_\infty = \frac{PR_C}{2\sigma_{f,\alpha} cos^2\alpha} \quad \text{(Eq 4.3)}$$

$$t_{90} = \frac{PR_C(2 - tan^2\alpha)}{2\sigma_{f,90}} \quad \text{(Eq 4.4)}$$

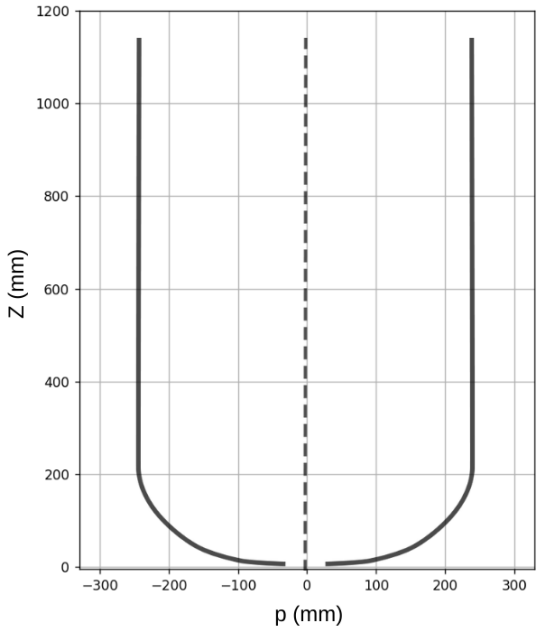

Figure 4.1: Reference graph for dome shape generation

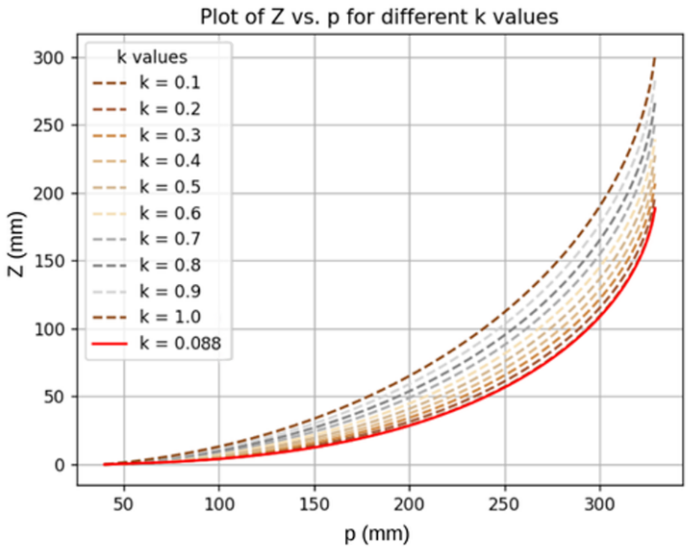

Figure 4.2: Dome Shape for T700S CF and diffrence in other curves

Solving the equations above yielded thickness values ranging from 33mm to 39mm. This variation arises because the python script shown in Appendix A.2, acting as the solver, considered several winding angles that range from 0 degrees to 55 degrees. Figure (4.3) illustrates the resulting relationship between hoop and helical thicknesses at different angles. Notably, a lower helical thickness would necessitate an increase in hoop layers to compensate.

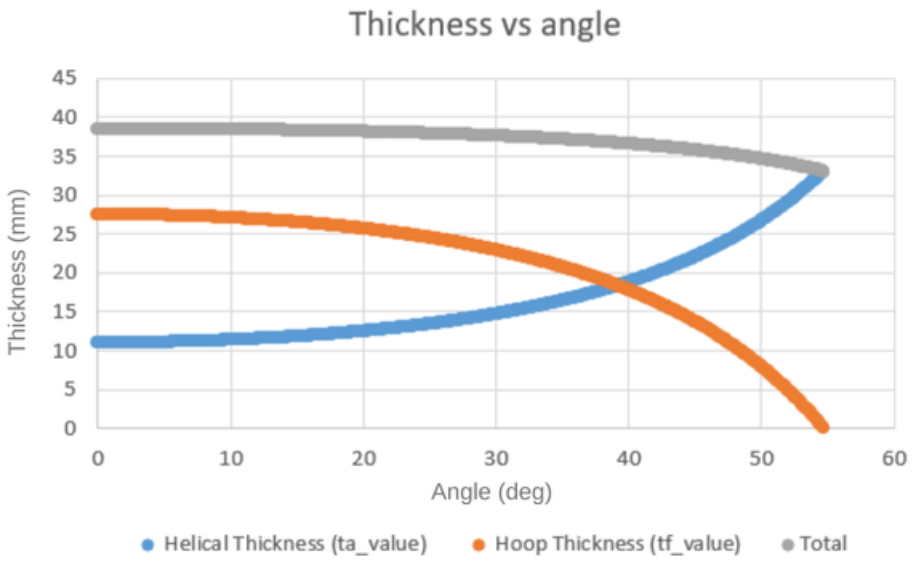

Figure 4.3: CF layer thickness vs Angle generated with the script A.2

4.3 Hydrogen tank design using Finite Element Analysis

1. **Dome shape and tank design**
   This step involved incorporating the generated dome geometry into Abaqus. The series of points defining the dome's surface were exported and used to create a sketch within the software (Figure 4.4). The cylindrical part of the tank was then added into this sketch. This, together with the finalized tank design was used to create a revolved solid within Abaqus (see Figure 4.5). The solid model was then revolved 180 degrees, representing a single quarter of the entire tank. By utilizing this approach, the final model represented a quarter shell of the tank, simplifying computational resources and reducing analysis complexity.

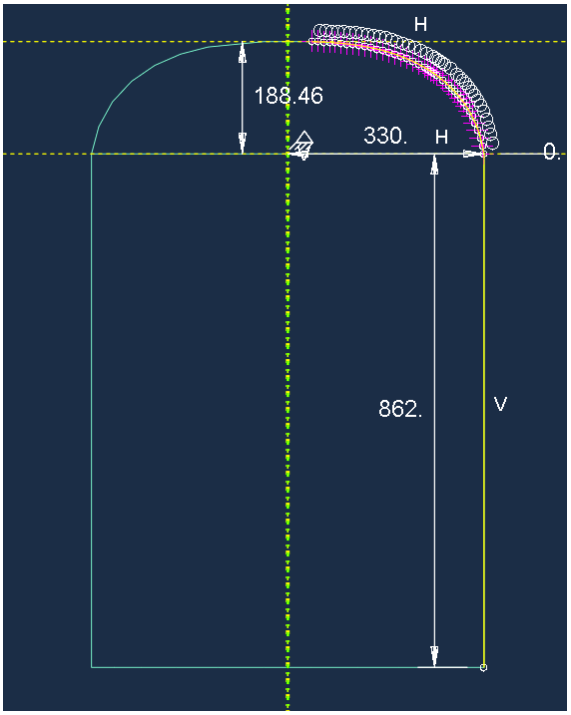

Figure 4.4: 2D sketch of the tank

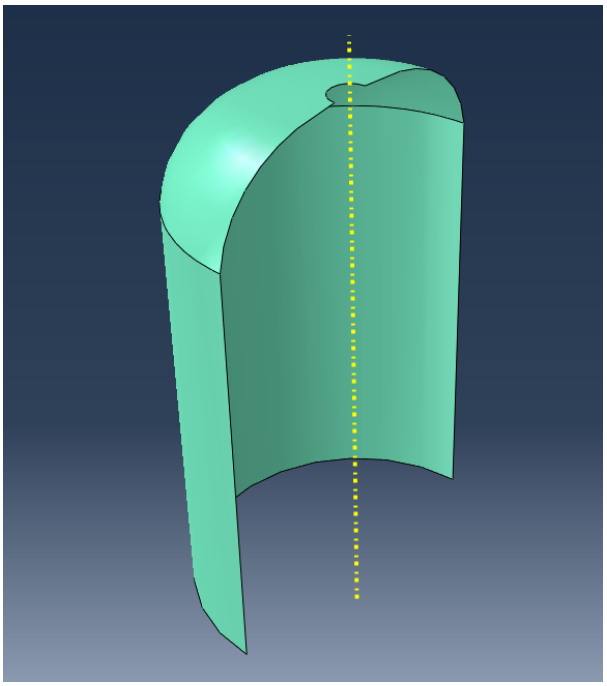

Figure 4.5: Quarter shell of the tank model

2. **Inner liner and carbon fiber composite layer**:
   To define the different materials within the model, two separate parts have to be created. The inner liner for this model is PA, also known as nylon. The outer layer represents a CF composite.
3. **Mechanical properties of the materials**
   After creating the inner and outer layer for the model. The next step was to specify the material properties for both the Nylon6 inner liner and the CF layer. The material properties can be seen below for T700S and the Nylon6 inner liner (Table 4.1). This is crucial for realistic simulations and these properties include Young's modules and Poisson's ratio (see section **4.2.1** for explanation).

Table 4.1: Material Properties of Hydrogen Fuel Tank Components

Symbol	Description	Value	Unit
	Carbon fiber composite		
E_1	Longitudinal modulus	135	GPa
E_2	Transverse modulus	9.66	GPa
ν_{12}=ν_{13}	Poisson's ratio (In-plane)	0.25	-
ν_{23}	Poisson's ratio (plane 2-3)	0.4	-
G_{12}=E_{13}	In-plane shear modulus	6	GPa
G_{23}	Shear modulus (planes 2–3)	3.5	GPa
	Nylon6 liner		
E_{PA}	Young's modulus	1.45	GPa
ν_{PA}	Poisson's ratio	0.3	-

4. **Mesh generation**
   Mesh generation is a critical step for accurate simulation results which involved discretizing the model's geometry. This was accomplished by creating a mesh, essentially dividing the model into small interconnected elements. The quality of the mesh affects the accuracy of the simulation results. Abaqus offered various meshing techniques and in this study, quadrilateral elements was chosen with a sweeping technique. This selection was based on the model's geometry and the level of detail that was desired. A global element size of 31 was used. While a finer mesh might have been ideal, limitations of the software prevented the use of smaller elements. However, it was determined that the current mesh was adequate for the analysis. The final mesh can be seen in Figure 4.6.

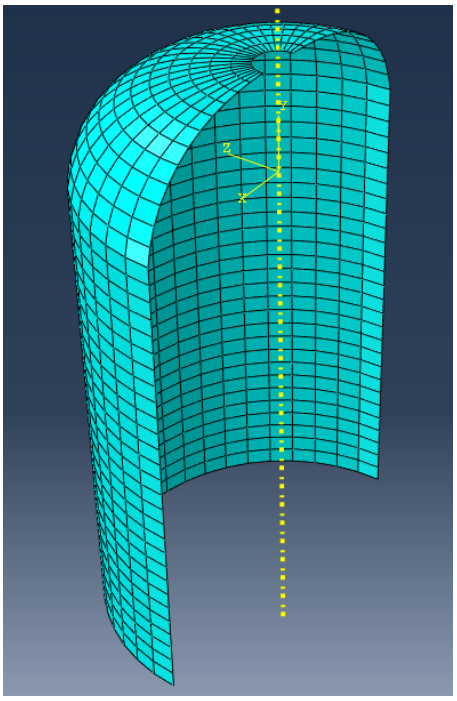

Figure 4.6: Meshed quarter shell of the tank model

5. **Boundary conditions and inner pressure**
   To achieve accurate results, the model incorporated boundary conditions that replicated real-life loading and deformation constraints. These conditions defined the model's interaction with its surroundings, such as simulating support structures and the allowed deformations during interactions(see Table 4.2 below for more information). Since the model represented one quarter of the entire tank, the following boundary conditions were specifically defined for this type of tank model:
   - **Y-direction constraint**: The bottom red line was fully restrained in the Y-direction (U2) (highlighted in Figure 4.7) to introduce reaction forces from the missing parts of the entire tank.
   - **Y-axis symmetry**: The same bottom red line shown in Figure 4.7 was decided to be the reference or mirror line and have a symmetrical shape along the Y-axis with the following conditions (U2=UR1=UR3=0).
   - **Z-axis symmetry**: As shown in the Figure 4.8, the highlighted line was decided to be the reference or mirror line and have a symmetrical shape along the Z-axis with the following conditions (U3 = UR1 = UR2 = 0).
   - **Kinematic coupling**: A point was created on the center axis at the boss section of the tank model as shown in 4.10. This point has the degree of freedom only on the Y axis, the point was only allowed to move on the Y-axis (U1=U3=UR1=UR2=UR3=0). This point is connected to the surface nodes of the tank model and the same condition as mentioned above is provided to the interaction between the surface nodes and the point. Thus the edge of the tank is allowed to displace only in the y-axis. This boundary condition will make the model stiff at that section but if this condition is not used the result will not be favorable as shown in the image 6.2
   - **Pin constraint**: A pin constraint was applied to one corner of the model, fixing it in all degrees of freedom (U1 = U2 = U3 = 0) to prevent deformation and ensure a stable reference point during analysis. This avoids singularity issues during evaluation.
   - **Loading condition**: A uniform pressure load of 70 MPa (700 bar) was applied to the inner surface of the tank model to simulate the maximum internal pressure conditions (see Figure 4.9). The pressure will reduce overtime when the fuel is consumed by the FCEV, but the storage unit will be designed with the maximum pressure condition.

Table 4.2: Boundary conditions

Symbol	Description
U1	Displacement in X-axis
U2	Displacement in Y-axis
U3	Displacement in Z-axis
UR1	Rotational displacement in X-axis
UR2	Rotational displacement in Y-axis
UR3	Rotational displacement in Z-axis

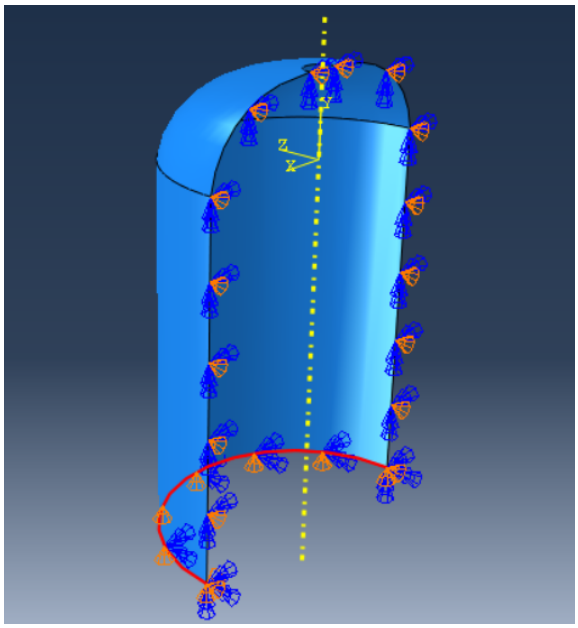

Figure 4.7: Boundary condition on the Y axis

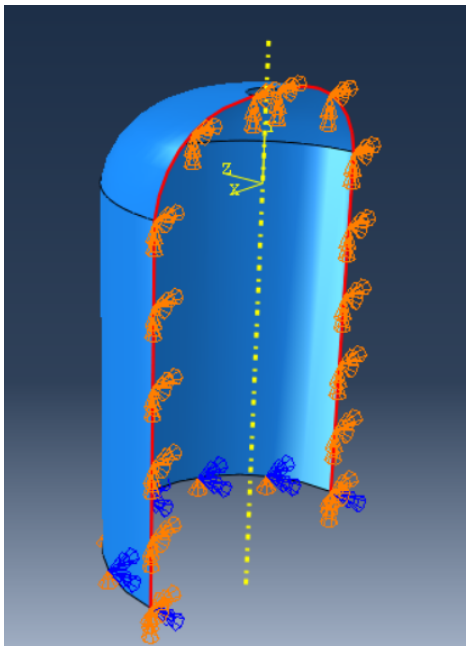

Figure 4.8: Boundary condition on the Z axis

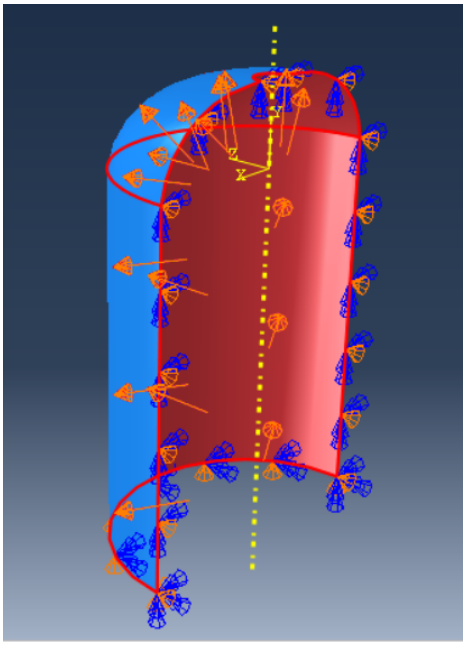

Figure 4.9: Inner pressure load

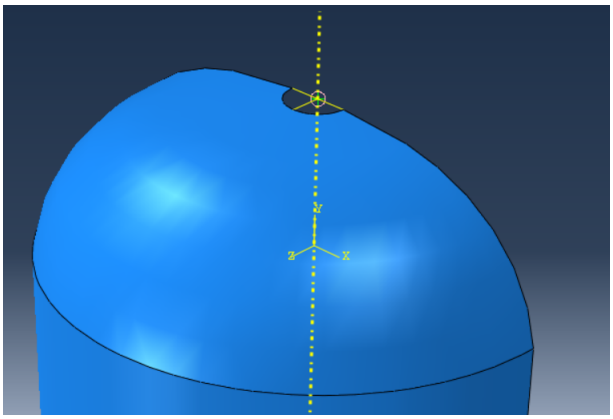

Figure 4.10: Boundary condition on the boss section

6. **Create helical and hoop plies**
   This step addressed specifying the CF layers within the composite material in Abaqus software. Two key ply orientations were adopted, helical and hoop plies. These ply orientations determined the material's response to stress, strength and stiffness, depending on the applied force direction. This therefore showcases an anisotropic behavior, where properties vary based on direction.

Furthermore, knowledge from prior DFMEA indicated that using only helical and hoop plies could lead to delamination due to the abrupt change in fiber angle between these layers. This was overcome by introducing an intermediate ply with an angle between the helical and hoop plies. This intermediate angle created a smoother stifness transition and reduced the risk of delamination. The CF layer thus comprised a combination of helical, intermediate, and hoop plies. The thickness of each ply was assumed to be 0.3 mm based on reference (Madhvi and et al, 2009). While the PA inner liner was assumed to be 5 mm. The next step involved defining the sequence, or order, in which these plies would be layered. An example sequence can be visualized in Table 4.3 and Figure 4.11. Furthermore, the selection of the region for each ply type was determined. For example, the hoop plies was only applied to the cylindrical portion of the model, while the intermediate and helical plies encompassed the whole model,

Table 4.3: Example of one ply sequence of the shell

		Ply Name	Region	Material	Thickness	CSYS	Rotation Angle	Integration Points
1	✔	Inner liner	(Picked)	PA12	5	<Layup>	0	3
2	✔	Hoop1	(Picked)	Composite	0.3	<Layup>	90	3
3	✔	Intermediate 1	(Picked)	Composite	0.3	<Layup>	60	3
4	✔	Intermediate 2	(Picked)	Composite	0.3	<Layup>	-60	3
5	✔	Helical 1	(Picked)	Composite	0.3	<Layup>	20	3
6	✔	Helical 2	(Picked)	Composite	0.3	<Layup>	-20	3
7	✔	Intermediate 3	(Picked)	Composite	0.3	<Layup>	60	3
8	✔	Intermediate 4	(Picked)	Composite	0.3	<Layup>	-60	3

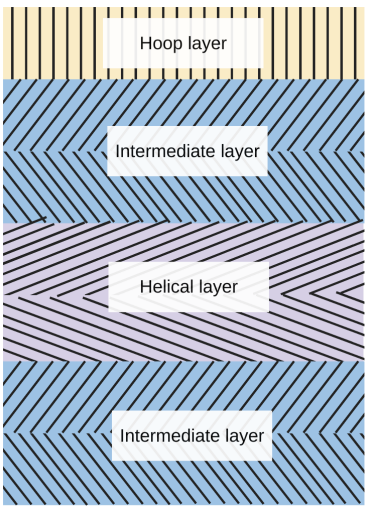

Figure 4.11: A cross-sectional representation of a ply sequence

7. **Run simulation and analyze results**
   Once all components were defined, the Abaqus simulation was initiated. The software solved the governing equations based on the chosen static analysis

type and the defined parameters. Upon completion of the simulation, the results were analyzed to evaluate various aspects of the design's performance under the simulated conditions. This analysis focused on several key metrics:

- **Factor of safety**: This metric shows how close the material was to failure under the loads applied. A target FOS of 2.25 was chosen for this analysis which is the fixed parameter.
- **Longitudinal stress**: This value represents the probability of material yielding under the given load. A maximum allowable stress of 1.271 MPa was established for every ply. This value was derived by dividing the material property (yield strength) of T700S CF (2.860 MPa) (Tooray, 2018) by the chosen FOS (2.25). This ensured the maximum stress remained within a safe limit for the tank.
- **Strains**: Based on the mechanical properties of CF composite, the maximum allowable strain at failure was 2.1% Tooray, 2018. Strains represent the internal forces and deformations in the material.
- **Mass**: From the results obtained regarding the stress and strain conditions of the composite tank as simulated by the Abaqus model, data on volume were extracted and fed into another code (see Appendix **A.1**). This code then calculated the mass of the entire tank, including both the CF and resin components. The code used material properties such as a density of 1.80 g/cm^3 for T700S CF (Tooray, 2018) and 1.73 g/cm^3 for the epoxy resin (Matweb, 2024). The volume fraction of the composite material used here is 60% of CF and 40% of resin as per the Tooray specification sheet (Tooray, 2018). Since the Abaqus model only represented a quarter of the actual tank, the volume obtained from the model was multiplied by 4 to determine the total volume while calculating the total mass.

4.4 Design of experiments

This chapter describes the iterative design process used to develop the final hydrogen tank design. A comprehensive explanation of the design methodology itself can be found in **section 3.3**. The focus here is on the outcomes achieved through this iterative approach. The process began with a DOE to evaluate the influence of various ply sequences and angles on the performance and mass of the tank. The DOE analysis informed both a subsequent trial-and-error optimization stage and a deeper understanding of the relationship between carbon fiber mass, design, and tank performance.

4.4.1 Sequence Testing

In the initial phase of the DOE, the goal was to understand how varying ply sequences affect the overall structural integrity. This was done by creating several models where the ply angles remained constant but the actual ply sequences differed. The layout for each sequence started with a single hoop layer, helical layers and then intermediate plies whose angle was placed between the two layers. The

number of intermediate and helical plies varied across the 5 sequences to assess their impact on the results (see Table 4.4). The picture below shows the 5 different sequences that were investigated. To facilitate a fair comparison, these sequences were multiplied until a total of nearly 80 plies was achieved. This process was repeated for different angles to identify if the optimal sequence would remain the same but also to evaluate the influence of angles on sequence selection.

Table 4.4: Different sequences with 52° angle on intermediate plies and 20° angle on helical plies

Seq 1	Seq 2	Seq 3	Seq 4	Seq 5
90	90	90	90	90
52	52	52	52	52
-52	-52	-52	-52	-52
52	20	20	20	52
-52	-20	-20	-20	-52
20	20	52	20	20
-20	-20	-52	-20	-20
52	20		52	20
-52	-20		-52	-20
52	52			52
-52	-52			-52
				52
				-52

To identify the optimal ply sequence, a stress and strain analysis was conducted. This analysis evaluated two key parameters across the different ply configurations. The first parameter was an average strain that considers the average deformation of all layers in both the cylindrical and dome sections of the tank model. This gave an overview of the general mode of deformation of the tank under pressure. The second parameter focused on the maximum stress experienced by the innermost helical and hoop layers. Since the innermost layer typically bears the maximum pressure in composite pressure vessels, this analysis was important to ensure that the critical layers remained within safe limits. The stress and strain are compared between each sequences in the following figures 4.12, 4.13 and 4.14. The analysis revealed the following key findings regarding the different ply sequences:

- **Sequence 1**: This sequence showed the lowest hoop stress because of the existence of more intermediate layers, which was confirmed by the plot of the hoop stress relation plot (see Figure 4.14). The reason for this is that intermediate layers are effective at mitigating hoop stress due to their high angles, resembling a dedicated hoop layer. However, it exhibited high helical stress. This characteristic makes Sequence 1 a good candidate for incorporating "doily layers" which can relieve helical stress while the intermediate layers manage most of the hoop stress.
- **Sequence 2**: This sequence achieved the lowest helical stress due to its higher amount of helical layers (see Figure 4.13). However, due to the higher amount of helical layers in sequence 2 it also suffered from the highest hoop stress among all sequences.
- **Sequences 3 and 5**: These two sequences displayed a balance between both helical and hoop stress. A relation could be found which is, if the stresses

on the helical layer was low the stresses in the hoop layer was high and vice versa depending on the angle. This relation between helical and hoop stress showed a good and balanced design, but the overall stress and strain values were found higher compared to Sequence 4.

- **Sequence 4**: This sequence exhibited the lowest overall strain while maintaining low stress, making it the best sequence (see Figure 4.12). The sequence showed a more balanced sequence of helical and intermediate layers which was similar to what was seen in sequences 3 and 5, but sequence 4 had more desirable outcomes overall.

Based on this analysis and the trends observed in the stress and strain graphs, it was clear that Sequence 4 was the most robust ply sequence. The sequence had a balanced composition of helical and intermediate layers and still provided good overall performance in terms of strain and stress distribution. Additionally, by increasing the intermediate layer angles it could further compensate for hoop layer stresses, as suggested by the trend in the hoop stress relation plot (see Figure 4.14). The analysis of various angles revealed that angles significantly influenced the stress values. However, the observed effect was proportional across different ply sequences based on the provided data. The stress changes followed the same trend for different sequences with respect to changing angles. This implied that a single, optimal ply sequence could be chosen regardless of the chosen angle.

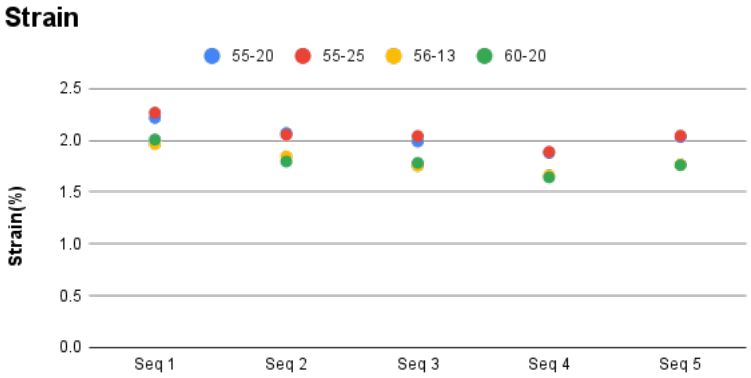

Figure 4.12: Strain relation for the different sequences

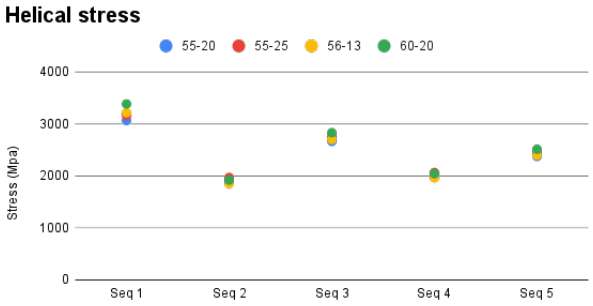

Figure 4.13: Helical stress (in Mpa) relation for the different sequences

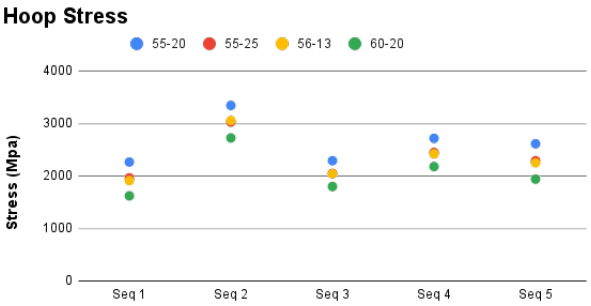

Figure 4.14: Hoop stress (in Mpa) relation for the different sequences

4.5 Ply Angle Testing

In the second phase of the DOE focused on evaluating how angles impacted strain and stress distribution within the two most promising sequences identified in phase one. These two sequences are sequence 4 and 1. To isolate and understand the effects of both helical and intermediate angles, a two-step process was employed:

1. **Helical angle analyse**: First, a range of helical angles (13°, 15°, 17°, 19°, 21°, 23°, and 25°) were tested while keeping the intermediate angle constant for each experiment in both sequences. The aim of this approach was to isolate and find the impact of only helical angles on stress distribution. The results can be visualized in the figures comparing average strain (Figure 4.15 and Figure 4.16) and helical stress (Figure 4.17 and Figure 4.18) for both sequences with varying helical angles.
2. **Intermediate angle analyse**: Following the helical angle analyse, the intermediate angles were varied (52°, 54°, 56°, and 57°) while maintaining a constant helical angle in both sequences. This variation allowed for observing only the influence of intermediate angles on stress distribution independent of helical angles.

Using this two-step process, it provided a clear understanding of how helical and intermediate angles both individually and in combination affected the strain and stress distribution within Sequences 4 and 1. The figures referenced earlier (Figures 4.15 to 4.20) allow for a detailed comparison of the effects on both sequences.

Stress analysis for sequence 1 and sequence 4

The analysis of stress response in each sequence revealed distinct trends:

- **Sequence 1**: The hoop layer stress decreased with increasing intermediate and helical angles, suggesting that higher angles for both layers contribute more to the hoop layer. The helical layer stress decreased slightly with decreasing intermediate angles, but changes in helical angles within this DOE model did not significantly impact its stress.
- **Sequence 4**: Similarly to Sequence 1, the hoop layer stress decreased with

increasing intermediate and helical angles, indicating once again a proportional relationship. However, in contrast to sequence 1 the helical layer stress in Sequence 4 increased with increasing intermediate and helical angles. This showed the need for a trade-off between managing hoop stress and helical stress in this sequence.

By analyzing the two sequences, it was revealed that balancing intermediate and helical angles for optimal stress distribution within the tank was of high importance. Additionally, varying the numbers of hoop layers across the plies can further improve design effectiveness. This was found by concentrating more hoop layers towards the inner ply section appeared to yield superior performance based on the findings. This can be seen in the table A.2 for the Design 1 ply layers that it has three hoop layers in the inner section of the CF layer and the amount of hoop layer decrease as it goes to the outward section of the CF layer.

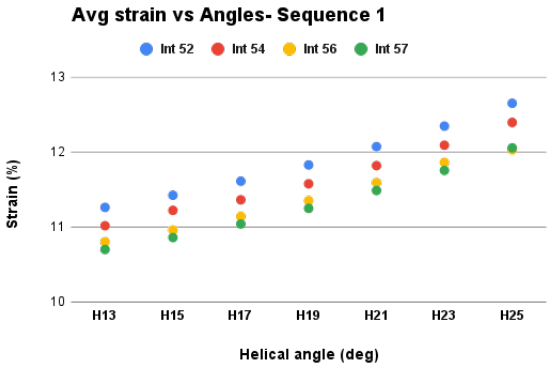

Figure 4.15: Average strain relation for sequence 1 with different angles

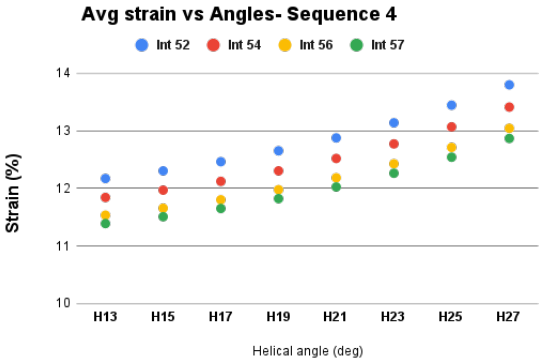

Figure 4.16: Average strain relation for sequence 4 with different angles

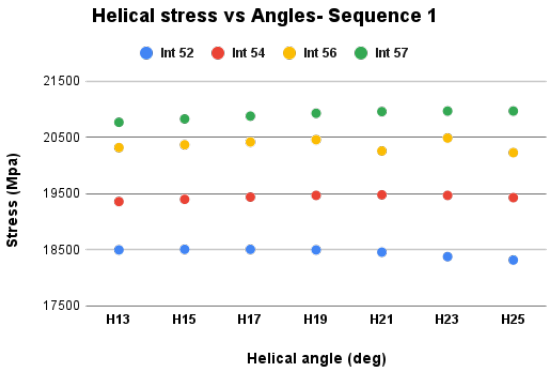

Figure 4.17: Helical stress relation for sequence 1 with different angles

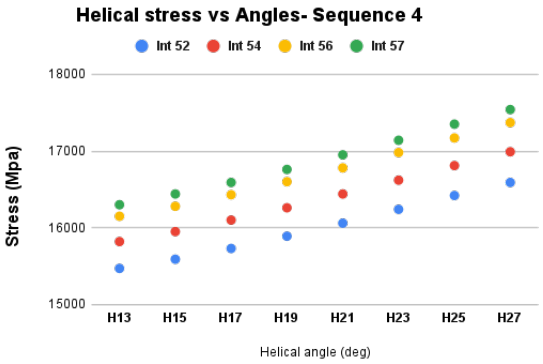

Figure 4.18: Helical stress relation for sequence 4 with different angles

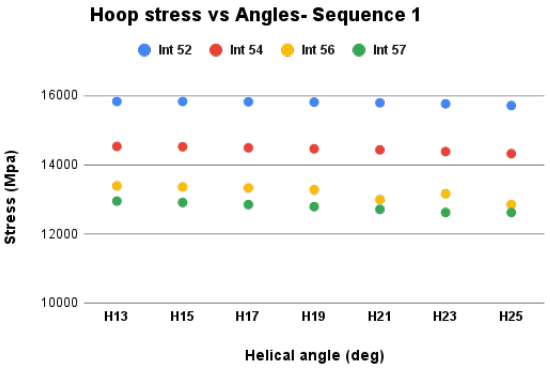

Figure 4.19: Hoop stress relation for sequence 1 with different angles

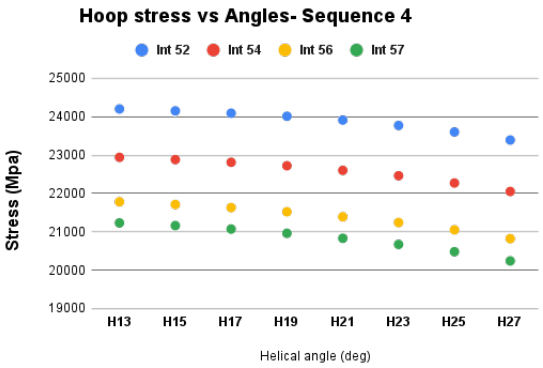

Figure 4.20: Hoop stress relation for sequence 4 with different angles

4.6 Empirical approach

An empirical approach was adopted to analyse the retrieved data from sequence and angle testing from the previous section (see Figure 4.21). This approach involved making assumptions and adopting a trial-and-error approach to identify the impact and relationship between various sequences and angles. The aim was to identify the optimal design based on the tank's stress, strain and mass. The other designs would then utilize the DfS strategy effective usage. This is because, by utilizing manufacture method like doilies, the design optimizes the placement of CF material. Doilies are strategically added in the tank at weaker places, through which reduction of overall CF can be done without any loss of stress. This minimizes material waste and promotes efficient resource utilization. The second DfS strategy utilized will be material selection. In this approach, some designs explore recycled CF as a potential material source. Using recycled materials reduces the environmental impact associated with virgin CF production, which could be intensive in both resources and energy.

Conditions if a ply fail and remedy to make it design safe
If Hoop fail

- Include intermediate ply angles greater than 50° in the overall sequence, such as 59°
- The variation in angle distribution, with lower intermediate angles like 50° in the inner layers and increasing to angles such as 59° in the outer layers, helps to distribute the stress evenly.
- Adding intermediate plies significantly reduces the hoop layer stress
- Lower hoop angle at the inner layers such as 70° and higher angles such as 90° at the outer layer
- Adding more hoop layer in a sequence at the inner layers of the tank and lesser hoop layers in a sequence at the outer layers of the tank

If Helical fail

- Have lower helical ply angles (<30°) (example 13°)
- Higher helical angle (example 30°) at the inner layers and lower angles (example 13°) at the outer layers to distribute the stress evenly
- Have lower intermediate ply angles (<58°) (example 50°)
- Adding intermediate plies significantly reduces helical stress in the cylindrical section, but has minimal effect in the dome section
- Adding hoop slightly reduces helical stress

If Intermediate fail

- Have lower intermediate ply angles (<59°) (example 51°)
- Lower intermediate angle (example 50°) at the inner layers and higher angles at the outer layer (example 59°) to distribute the stress evenly
- Adding hoop significantly reduces intermediate stress

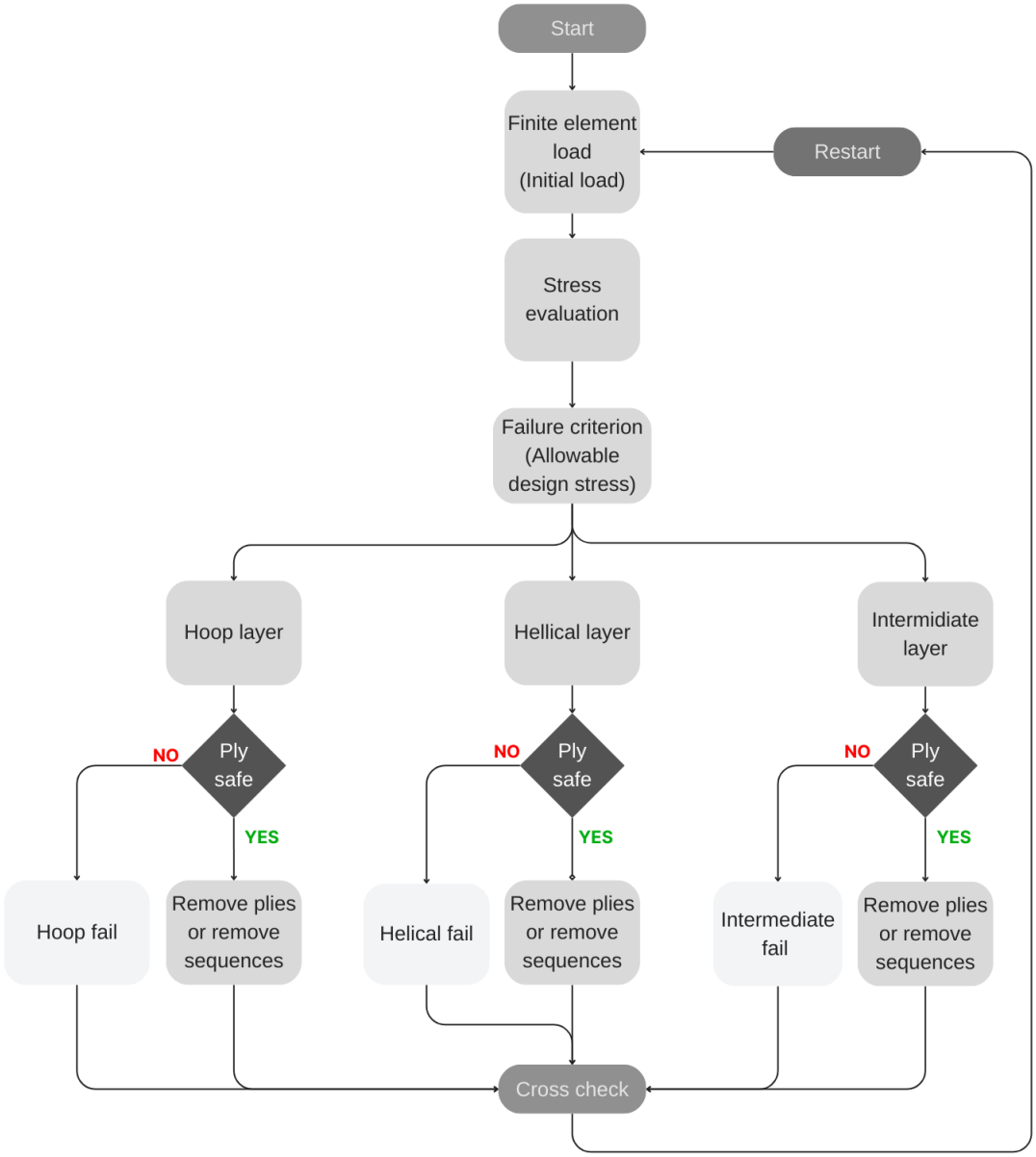

Figure 4.21: Trial-and-error approach for FEA

4.6.1 Angle optimization

The design of ply angles played a crucial role in managing stress distribution within the tank wall. The angles were chosen based on:

- **Hoop Layers**: Hoop layers were assigned 85 degrees instead of 90 degrees. Winding them at a full 90 degrees would not be practical. Additionally, a slightly lower angle at the innermost layers allows them to carry less stress, transmitting it progressively outwards. This strategy distributes stress more evenly across the entire tank wall meaning higher angles for the outermost layers and lower angles for the innermost layers.

- **Intermediate and Helical Angles**: Similar principles were applied to the intermediate and helical angles. The final design used higher angles for the innermost layers and lower (steeper) angles for the outermost layers. This approach promoted a more even stress distribution throughout the tank, reducing stress concentration and the peak stress experienced by the innermost layer. As a benefit, it also allowed for a reduction in the total number of plies needed, ultimately leading to a lighter tank design.

The order of angles within a sequence also proved to be critical. For example, using the same angle(40 degrees) for consecutive plies was found to be inefficient. The first ply would bear the brunt of the stress, leaving the second ply with minimal stress. A more effective approach utilized a lower helical angle in the preceding layer. However, this difference in angles needed careful consideration. If the difference was too large, the layer with the lower angle would carry an excessive amount of stress, compromising safety. The chosen design ensured that the difference in angles progressively increased as we moved towards the outermost layers. Since these layers experience lower overall stress, their angles were adjusted to encourage them to bear a larger share of the load, thereby reducing the burden on the inner layers (see Table 4.5 for one example of a sequence).

Table 4.5: Example of one ply sequence of the layer where the 40 degrees takes up more stress

Hoop1	85
Hoop2	-85
Hoop3	-85
S1-Interm 1	59
S1-Interm 2	-59
S1-Hellical 1	40
S1-Hellical 2	-40
S1-Hellical 3	40
S1-Hellical 4	-40
S1-Interm 3	59
S1-Interm 4	-59
Hoop4	85
Hoop5	-85
Hoop6	-85
S1-Interm 5	59
S1-Interm 6	-59
S1-Hellical 5	40
S1-Hellical 6	-40
S1-Hellical 7	40
S1-Hellical 8	-40
S1-Interm 7	59
S1-Interm 8	-59

5
Result

This chapter discusses the results of the design iterations for a CF pressure vessel. Seven different designs were created and analyzed using Abaqus software. Each design explored different factors such as material properties, winding and reinforcement strategies. The chapter also presents an inventory of the designs which includes the amount of CF material required, the type of recycled material used and additional energy consumption during the manufacturing process. Overall, the chapter investigates ways to optimize the design of a pressure vessel to reduce the environmental impact by using less CF and potentially recycled materials.

5.1 Final designs

This section explores seven design iterations for a CF component. Each design was created and evaluated using Abaqus software. The focus was on how changes in material properties, ply count, and ply angle affect the amount of CF needed and the stress distribution within the part. Line graphs are presented to visualize these comparisons. Although all designs share a common base structure, specific parameters like ply number and orientation were strategically modified to optimize factors like weight and stress distribution. For further information on the sequences and angles see Appendix (A.2, A.3).

5.1.1 Design 1: Base design

With mass reduction as one of the goals, which is the process of reducing the weight of a structure or component while maintaining its strength, functionality, and performance. This mainly involves detecting and eliminating extra materials in the design and optimizing load distribution. This optimization can be achieved by changing ply angles, angle distribution, ply sequence, and the amount of plies used. By doing so, a design was created with 163.19kg of vCF in the tank that can store 17kgs of gaseous Hydrogen, which is the base design in this experiment. The hoop layers were kept 85° in the inner layer and 90° at the outermost layer, while manufacturing it should be as close to 90° but due to manufacturing constraints it cannot be 90°. The intermediate angles were chosen to be 58° in all layers and the helical angles were from 40° in the inner layers to 13° in the outer layers. The stress results are plotted below in Figure (5.1). Each line represents a single ply layer of the composite material, which is made of 60% volume fraction T700s CF and 40% volume fraction epoxy resin. These plies are considered safe as long as the stress remains

below the dashed line indicating the 1271 MPa stress limit. The intermediate plies exceed the stress limit due to a modeling error explained in the discussion chapter. The green, red, and blue lines represent the stress in the S11 direction which are the longitudinal stresses for each ply layer. The ply sequence layout for this design is shown in A.2

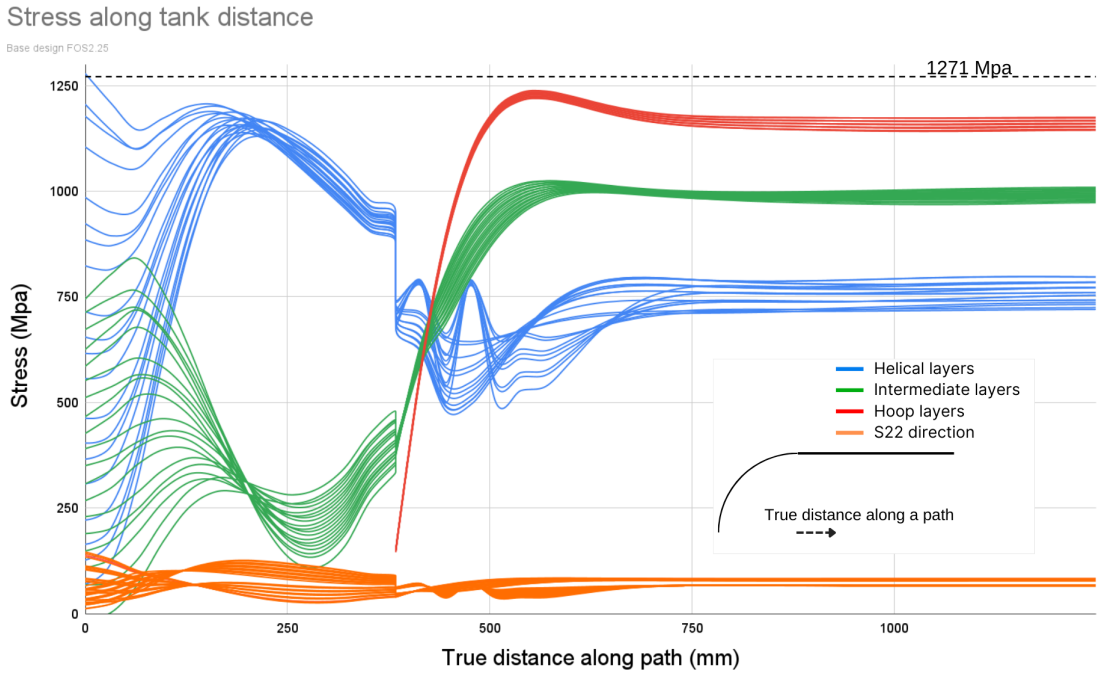

Figure 5.1: Stress results for tank design 1

5.1.2 Design 2: rCF-Microwave Pyrolysis

From the base design, the material is swapped from vCF to rCF by changing the mechanical properties. The rCF used here is by the recycling process called microwave pyrolysis, which has 99.6% with regards to the tensile strength and 118% of the stiffness when compared with vCF (Kaliswal, 2024). The design allowable stress is 1258 Mpa and stiffness is 1.18 times higher in E1, E2 and E3. The stress across the tank is plotted for this design as shown in 5.2. The ply sequence layout for this design is shown in Appendix (A.2)

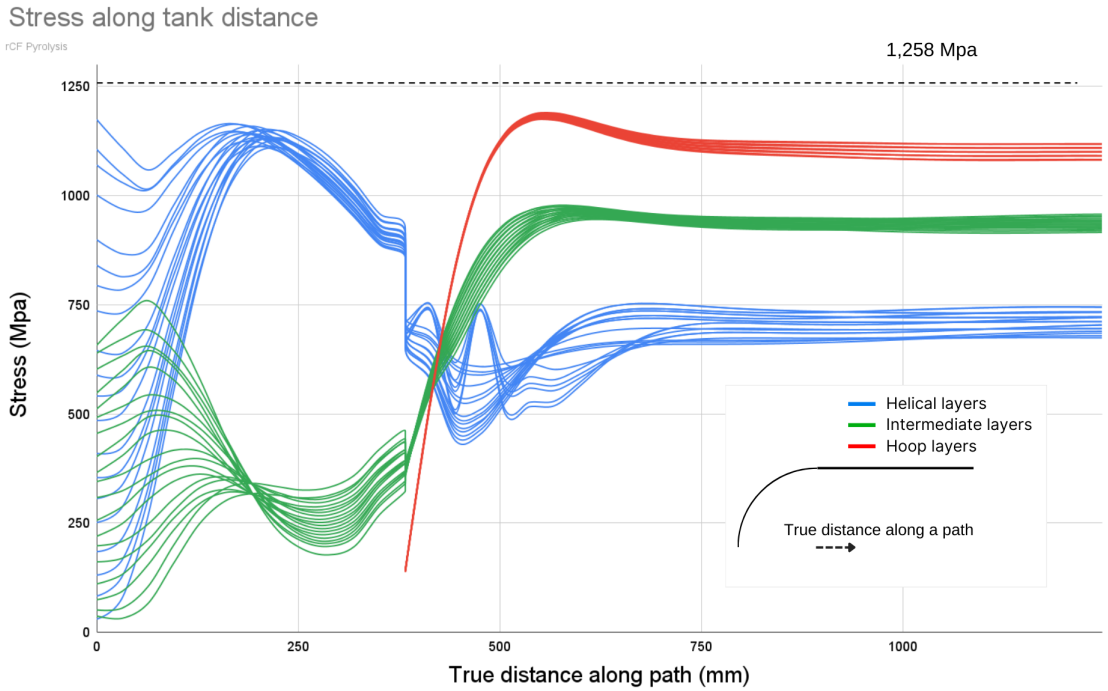

Figure 5.2: Stress results for tank design 2 - rCF Microwave Pyrolysis

5.1.3 Design 3: rCF-Solvolysis

The base design underwent a material substitution, switching from vCF to rCF. This change involved modifying the mechanical properties within the design software. The specific rCF utilized employs a solvolysis recycling process, boasting tensile strength retention of 98.9% and stiffness retention of 100% compared to vCF (Kaliswal, 2024. Since the design aims to maintain stiffness, the design allowable stress was set at 1245 MPa. The stress distribution across the tank for this rCF design is depicted in Figure (5.3). Additionally, the corresponding ply sequence layout for this design is shown in Appendix (A.2).

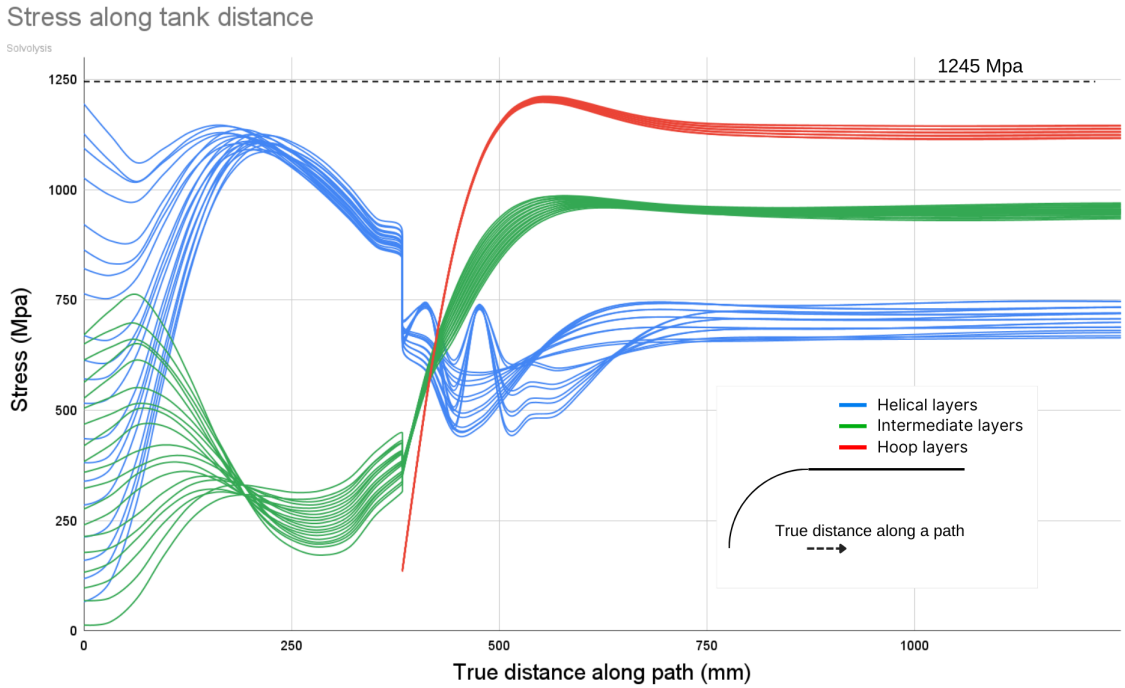

Figure 5.3: Stress results for tank design 3 - rCF Solvolysis

5.1.4 Design 4: rCF-Solvolysis in hoop layers

The same rCF-Solvolysis material is used in this design, only the hoop layers are replaced with the rCF material but the helical and intermediate layers will remain the same. The stress across the tank is plotted for this design as shown in Figure(5.4). The black dotted line indicates the allowable stress for the vCF and red dotted line indicates the allowable stress for the rCF. The ply sequence layout for this design is shown in A.2.

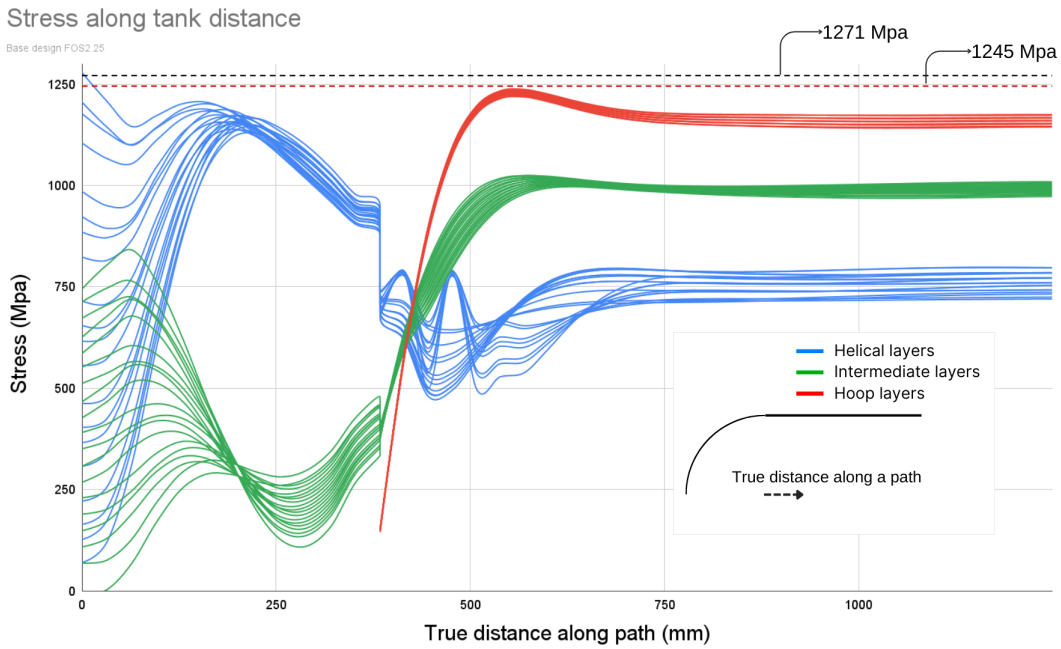

Figure 5.4: Stress results for tank design 4

5.1.5 Design 5: Patch reinforcement

This design employed patch reinforcement, also known as doily layers. These layers served a critical purpose: absorbing stress from the dome section of the tank, thereby alleviating the burden on the helical layers. The analysis conducted revealed that while the helical layers did contribute to managing stress in the dome section, as shown in Figure (5.5), their effectiveness in the cylindrical part of the tank was significantly lower. This finding indicated inefficient material usage in this area. To address this inefficiency, a strategy of strategically adding doily layers were implemented. This approach allowed for a certain amount of helical material to be removed, leading to a substantial reduction in tank mass. The conducted design demonstrated a successful mass reduction of 11.63 kg compared to the base design. The stress distribution across the tank for this design with patch reinforcement is shown in Figure 5.6. The corresponding ply sequence layout for this design is provided in Appendix (A.3).

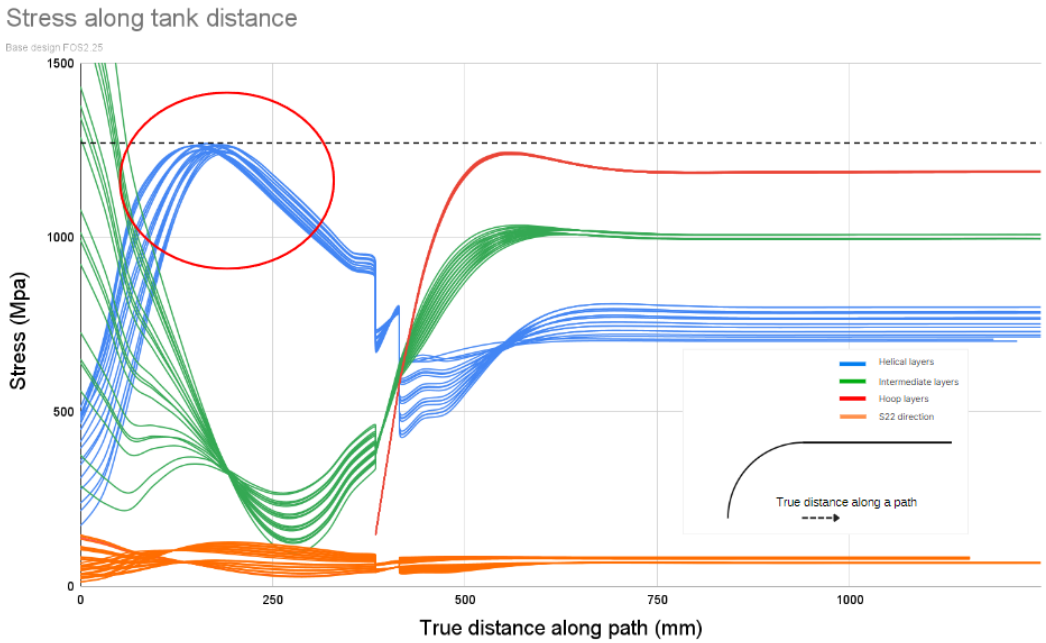

Figure 5.5: Stress taken by the helical layer in the dome section

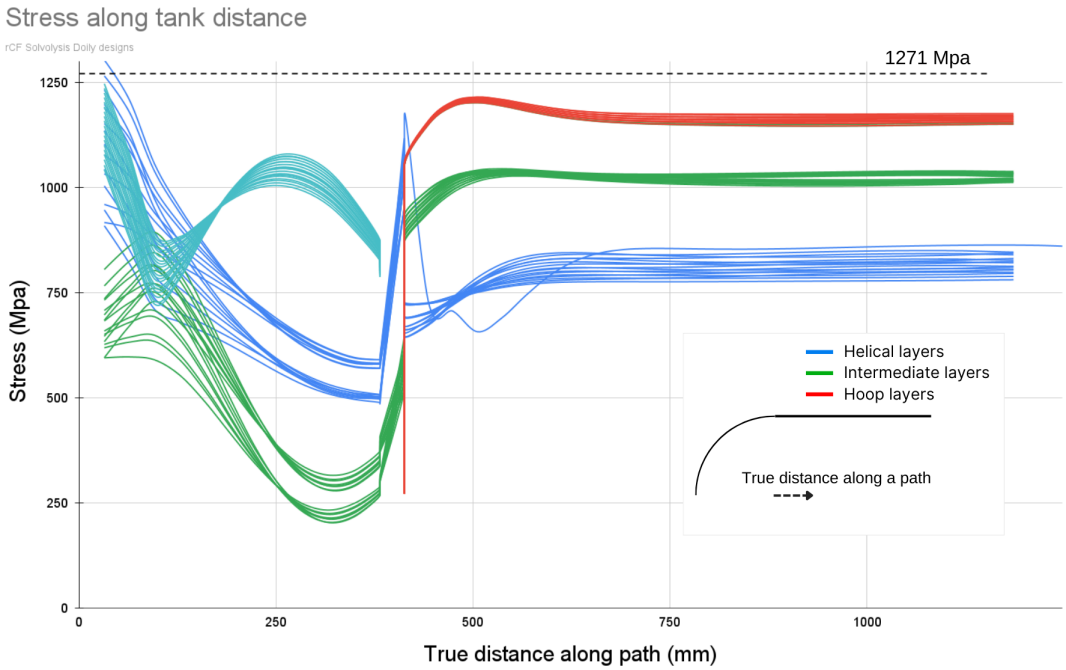

Figure 5.6: Stress results for tank design 5

5.1.6 Design 6: rCF-Solvolysis used in Patch reinforcement

The study investigated the feasibility of using rCF in doily layers due to the shorter fiber lengths produced with current recycling technologies. As a result, the doily layers in the previous design were replaced with rCF obtained through solvolysis

process. The resulting stress distribution for this design is shown in Figure (5.7). The black dotted line indicates the allowable stress for the vCF used in the base design, while the red dotted line represents the allowable stress for the rCF. The corresponding ply sequence layout for this design utilized rCF doily layers is provided in Appendix (A.3).

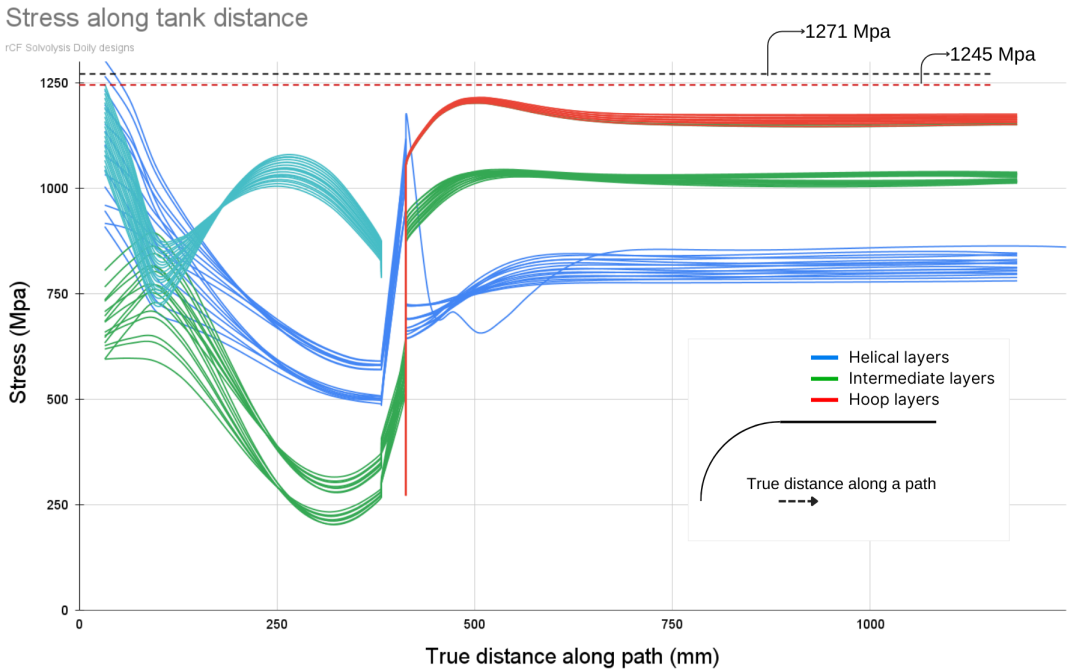

Figure 5.7: Stress results for tank design 6

5.1.7 Design 7: Base design FOS2

Future industry standards anticipate a reduction in the design FOS from 2.25 to 2 by the year 2027 (ISO, 2018). This change allowed to utilize a higher allowable stress limit in the design, consequently reducing the amount of CF required. The base design utilized a FOS of 2.25 necessitated 163.19 kg of CF. By reducing the FOS to 2 (designated as FOS2 base design), the optimized design achieved a weight reduction, requiring only 151.56 kg of CF based on the conducted experiments. The design process involved the incremental removal of layers until the stress limit was reached. This approach suggests the potential for further mass optimization, as illustrated in Figure (5.8). The corresponding ply sequence layout for this lighter design is presented in Appendix (A.3).

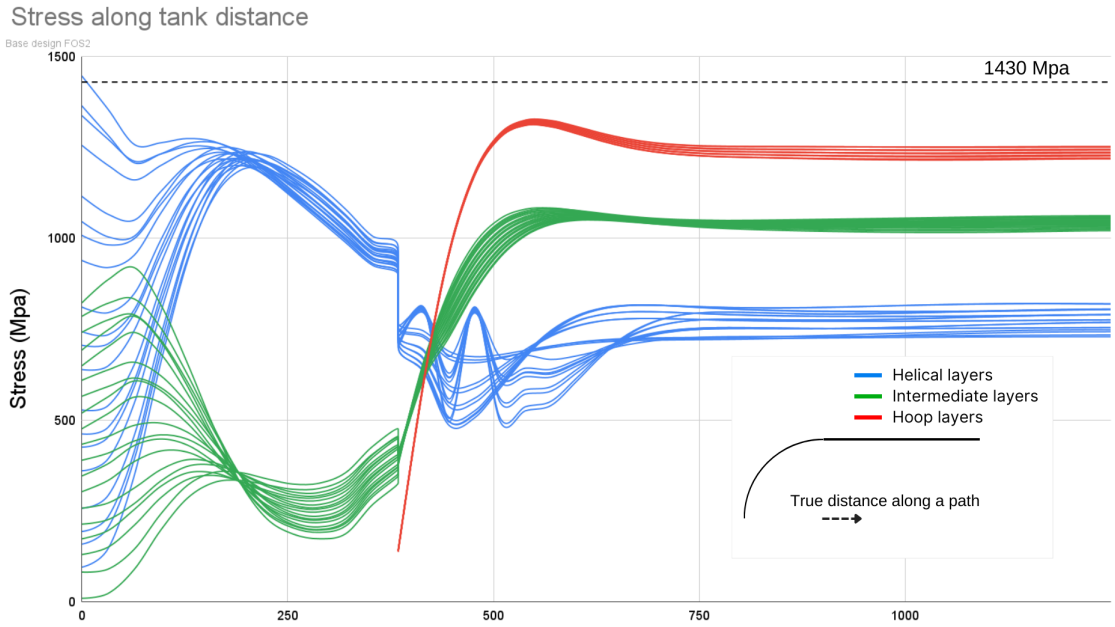

Figure 5.8: Stress results for tank design 7

5.1.8 Design 8: rCF-Solvolysis

Building upon the FOS2 base design (represented as Design 7 in the previous section), this design investigated the feasibility of replacing the virgin CF with recycled CF obtained through the solvolysis process. This substitution resulted in Design 8. The stress distribution for this design utilized rCF doily layers is shown in Figure (5.9). The corresponding ply sequence layout for Design 8 is provided in Appendix (A.3).

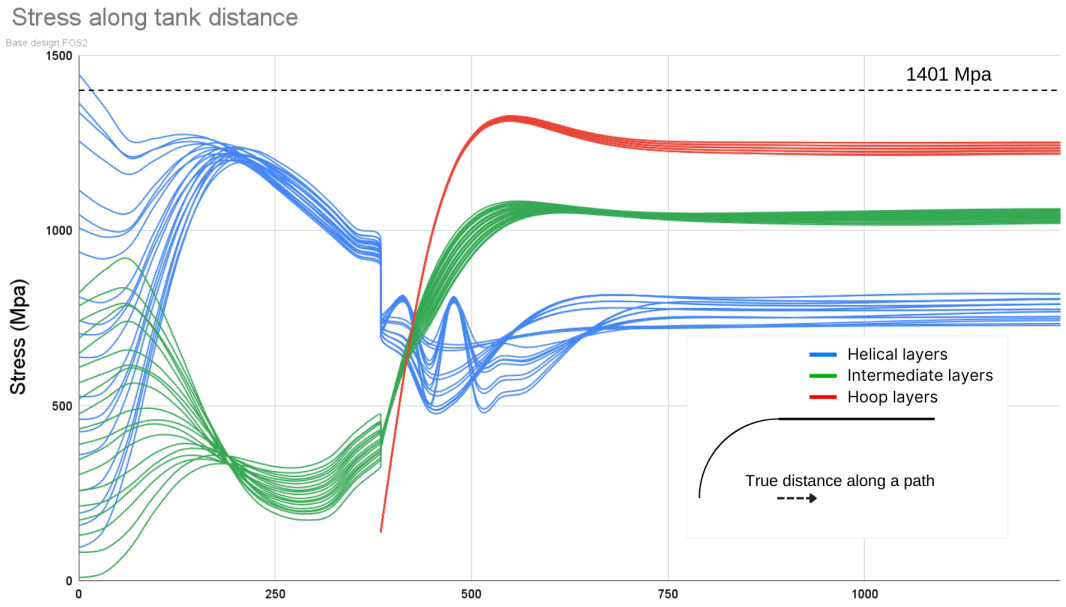

Figure 5.9: Stress results for tank design 8

5.2 Life Cycle Inventory (LCI)

The designs results are laid out in terms of material mass, the energy required from conventional wet winding process and the type of recycled material used. The designs produced are to be manufactured using dry winding process, which requires an energy (MJ) to store the prepreg CF spools in a cold storage that is used, shown as "C" in the Table 5.10, R is the energy required for the robotic arm to place the patch reinforcements on the mandrel. For an LCA, the table 5.10 can be utilised to compare the environmental impacts of the designs and here the energy "C" is not calculated since all the designs have that in common.

Table 5.1: Life Cycle Inventory (LCI) of the tank designs

Design	FOS	Energy	vCF (kg)	rCF (kg)	rCF type	Resin (kg)	Total weight(kg)
1	2.25	C	163.19	0	-	120.41	283.6
2		C	0	166.16	MR pyro	122.31	288.47
3		C	0	166.16	Solvo	122.31	288.47
4		C	136.55	26.96	Solvo/MR pyro	120.41	283.92
5		C + R	151.56	0	-	112.97	264.53
6		C + R	144.72	6.84	Solvo	112.97	264.53
7	2	C	151.56	0	NA	113.22	264.78
8		C	0	151.56	Solvo	113.22	264.78

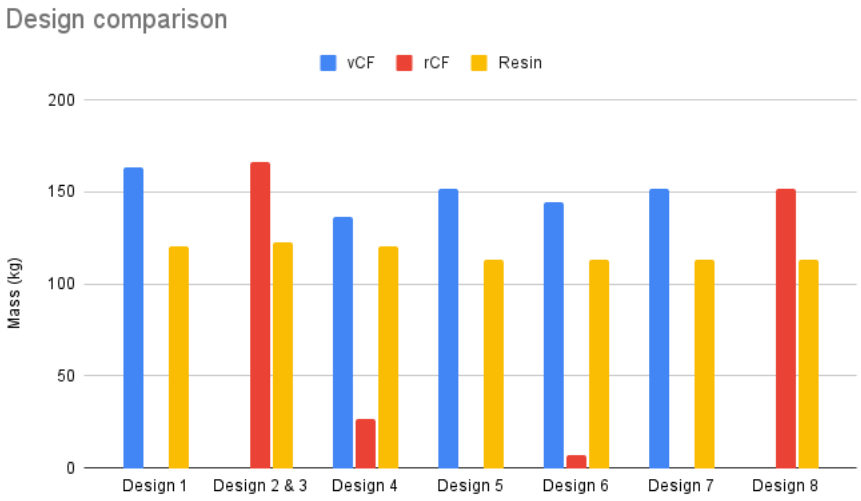

Figure 5.10: Design comparison with respect to mass of Carbon fiber in the tanks

6
Discussion

This chapter builds on the previously presented results and elaborate the potential errors in the model that might have affected the outcomes. A critical analysis was conducted to determine the significance of these error sources and their impact on the interpretation of the findings. Furthermore, the chapter explored the necessity of considering and accounting for these error sources in the design and execution of future projects.

6.1 Modeling error

In the Abaqus model, the CFs terminate abruptly at the boss section, which is the red region in the figure 6.2. This abrupt termination leads to stress concentration in that area, as depicted by the green lines in the stress graph 6.1, where the stresses in the intermediate plies exceed the stress limit of 1271 MPa. Kinematic coupling was employed to address this stress concentration; however, the fibers are still modeled to terminate abruptly at the boss section. Although this boundary condition increases the stiffness of the fibers in the affected area, mitigating the false stress, it remains an improper modeling approach.

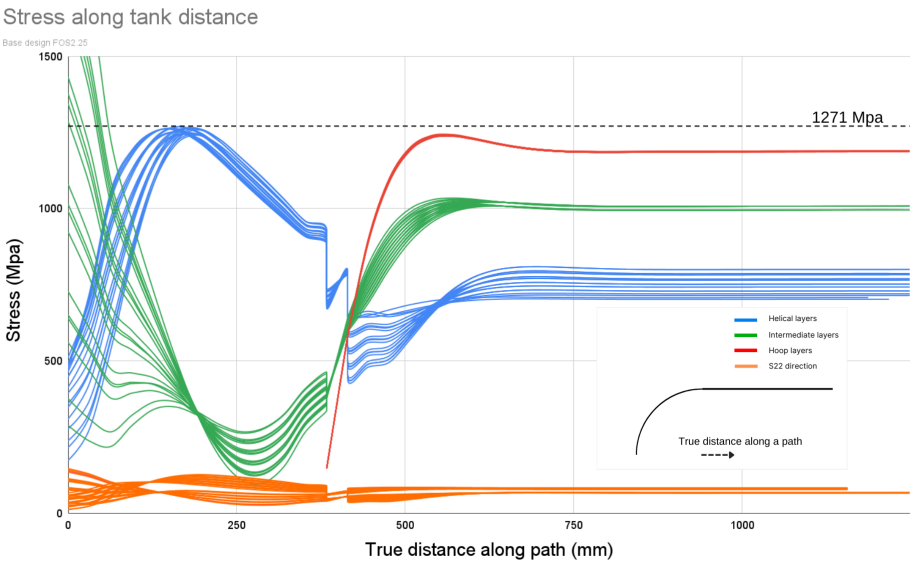

Figure 6.1: Stress result without Kinematic coupling

In reality, the composite fibers smoothly wrap around the boss structure during man-

ufacturing. This would then instead form a thin reinforcing layer and the wrapping action distributes stress more evenly throughout the fibers, as shown in Figure 6.3 (while this figure depicts a Type III tank, the CF cross-section would be similar in Type IV tanks). Moreover, the boss structure adds material due to fiber wrapping. This is not accounted for by the current model, which will under-predict capacity in the material at that region and produce incorrect stress predictions. However, the stress predictions in the dome and cylinder sections of the intermediate layers are likely more reliable. To allow for the lack of material in the region around the boss, the effective thickness there might be taken as being about twice the thickness of the dome section. This effectively increases the true stress experienced by the material. The true stress can be calculated by multiplying the maximum stress obtained from the simulation by the ratio of the effective thickness to the dome thickness. Following this approach, assuming the effective thickness is twice the dome thickness, the true stress would be: True stress = 1783 MPa x (1 / 2) = 891.5 MPa The fact that this adjustment has worked demonstrates that the design is still safe, but it does point to shortcomings of the existing Abaqus model.

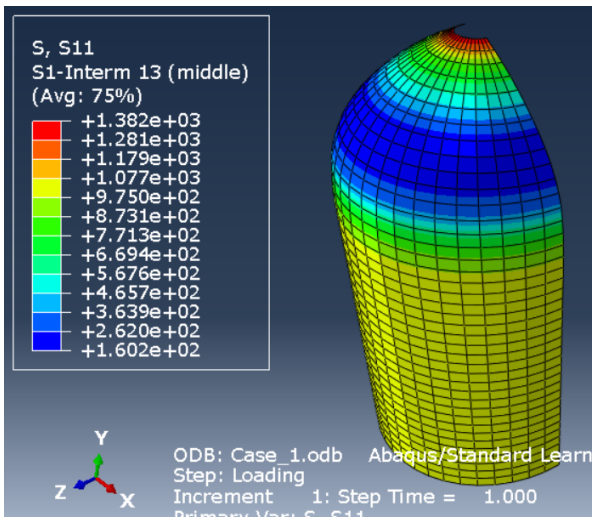

Figure 6.2: Error in the intermediate layer

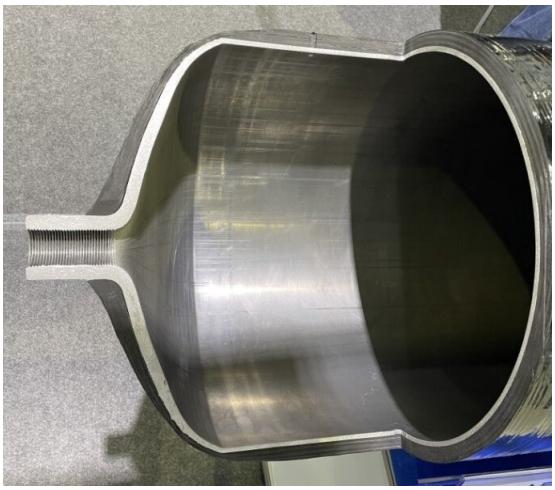

Figure 6.3: Cross section of type 3 tank

7
Future work

This chapter explores potential avenues for future research building upon the findings presented in this work.

7.1 Fatigue analysis

This design could be further tested for any influences of material reduction. One possible route of investigation is to research ways of reducing the number loading cycles the tank receives over its lifetime. This could be achieved by analysing typical use cases and identifying opportunities such as optimizing refueling procedures to minimize pressure fluctuations and stress variations within the tank. Another approach involves conducting a fatigue analysis to understand the trade-off between lifespan and material usage. This involves modeling accurately the growth of fatigue cracks under different loading conditions and safety analysis. The design could be tested by collaborating with a supplier to prototype a tank featuring the new design.

7.2 Material and shape change study

Alternative Carbon Fibers: Although the current design utilizes T700 carbon fiber, analyzing tanks manufactured with either T300 or T800 may reveal a more sustainable choice. T300 might be a more cost-effective option and have lower energy requirement since T300 requires less temperature to produce compared to T700, but its lower strength might necessitate a thicker tank wall, potentially negating any environmental benefit. On the other hand, T800's has higher tensile strength thus lesser Carbon fiber is required, which could allow for a thinner tank thus reducing the overall material use. However, its production process might have a higher environmental impact, requiring a careful evaluation of the strength-sustainability trade-off.
Remoldable resin: Currently, the tank utilizes a non-remoldable resin. Identifying the right thermoplastic resin could give the tank the possibility to be reshaped for a second use. This would significantly reduce the environmental burden associated with material production and disposal, promoting a more circular life cycle for the tank.
Natural Fiber Composites: Research into the viability of using natural fibers such as flax or hemp with carbon fiber could make a significant improvement in environmental impact. Generally, most of these natural fibers have a far lower environmental impact compared to carbon fiber. However, their mechanical properties

and durability are typically lower. Research into optimizing fiber blends and addressing these challenges is crucial for successful implementation of this potentially sustainable approach.

Different shapes of tank: Since the cylindrical structures are not that efficient in design space, exploration into the possibility of using honeycomb structure may be viable in storing gaseous hydrogen. Honeycomb designs with their non-cylindrical form could probably hold a gaseous load effectively.

8

Conclusion

This chapter builds upon the methodology for designing hydrogen fuel tanks for circularity and sustainability outlined in (**section 3.3**). This methodology focused on minimizing carbon fiber usage within the tank through optimized layer configuration and the potential incorporation of doilies and recycled carbon fiber.

As discussed previously, achieving an optimal stress distribution across all plies in the carbon fiber tank design is crucial. The ideal scenario involves a uniform stress profile below 1271 MPa throughout every ply. This not only maximizes fiber utilization but also promotes a sustainable design approach. As explained in the results section (**chapter 4 and 5**), achieving this optimal distribution necessitates precise placement of winding angles, a well-defined ply sequence, and the strategic use of patch reinforcement. While patch reinforcement might represent a more expensive solution, their potential to reduce carbon fiber usage by 7.16% (11.6 kg) in the current design and a staggering 58.4 kg for a five-tank vehicle makes them a highly sustainable practice. Thus making this a very effective strategy and a manufacturing method to reduce the mass of virgin carbon fibers in the tank.

The possibility of incorporating recycled carbon fiber into future iterations appears promising, especially with advancements in technology enabling the production of longer fibers. However, fatigue analysis becomes critical when using rCF due to potential micro-cracks and fiber degradation. This study demonstrates that initial and static loading conditions, even with a slight decrease in rCF tensile strength, can be addressed through a corresponding increase in the FOS. Another near-future design proposal involves utilizing shorter rCF specifically within the patch reinforcement. Hence, encouraging organizations to utilize rCF in the new tanks that are to be produced.

Another conclusion is drawn that if Volvo Trucks Technology implement the new manufacturing method, patch reinforcement will be needed. The tank would reduce the usage of vCF and also the possibility of using recycled carbon fiber in the tank would make the storage unit of the FCEV and the whole vehicle towards a more sustainable transport system.

Bibliography

Addcomposites. (2022). Filament winding hydrogen tanks (thermoset). https://www.addcomposites.com/post/filament-winding-hydrogen-tanks-thermoset#viewer-20i6

Azeem, M., & et al. (2022). Application of filament winding technology in composite pressure vessels and challenges: A review. https://www.sciencedirect.com/science/article/pii/S2352152X2101152X

Barthelemy, H. (2017). Hydrogen storage: Recent improvements and industrial perspectives. https://www.sciencedirect.com/science/article/abs/pii/S0360319916305559

Benitez, A., & et al. (2021). *Ecological assessment of fuel cell electric vehicles with special focus on type IV carbon fiber hydrogen tank* [Available 2021]. https://www.sciencedirect.com/science/article/pii/S0959652620333229#cebib0010

Billing, L. (2021). Circular economy is not the panacea many had hoped for. https://www.lunduniversity.lu.se/article/circular-economy-not-panacea-many-had-hoped

Böckin, E., Willskyt, S., Andre, H., Tillman, A., & Söderman, M. (2020). How product characteristics can guide measures for resource efficiency — a synthesis of assessment studies. https://www.sciencedirect.com/science/article/pii/S0921344919304884?ref=pdf_download&fr=RR-2&rr=860c89775abf8f5a

Christiansen, B. (2024). Bill of materials (bom) meaning, purpose, and types. https://limblecmms.com/blog/dfmea-pfmea/

DragonPlate. (n.d.). What is carbon fiber? https://dragonplate.com/what-is-carbon-fiber

Energy.Gov. (n.d.-a). Hydrogen fuel basics. https://www.energy.gov/eere/fuelcells/hydrogen-fuel-basics

Energy.Gov. (n.d.-b). Hydrogen production: Electrolysis. https://www.energy.gov/eere/fuelcells/hydrogen-production-electrolysis

Energy.Gov. (n.d.-c). Hydrogen production: Natural gas reforming. https://www.energy.gov/eere/fuelcells/hydrogen-production-natural-gas-reforming

Energy.Gov. (n.d.-d). Hydrogen storage. https://www.energy.gov/eere/fuelcells/hydrogen-storage

Foundation, E. M. (2021). What is a circular economy? https://www.ellenmacarthurfoundation.org/topics/circular-economy-introduction/overview

Gencer, E. (2021). Hydrogen. https://climate.mit.edu/explainers/hydrogen

Grant, M. (2023). Bill of materials (bom) meaning, purpose, and types. https://www.investopedia.com/terms/b/bill-of-materials.asp

Hermansson, F., Heimersson, S., Janssen, M., & Svanstrom, M. (2022). Can carbon fiber composites have a lower environmental impact than fiberglass? https://www.sciencedirect.com/science/article/pii/S0921344922000829

Hyfindr. (2024). Hydrogen tank – type i-iv. https://hyfindr.com/en/hydrogen-knowledge/hydrogen-tank

ISO. (2018). Svenska standard iso 19881:2022. https://www.sis.se/en/produkter/chemical-technology/products-of-the-chemical-industry/gases-for-industrial-application/ss-iso-198812022/

ISODIS. (2024). Iso dis 19881. https://www.iso.org/standard/82595.html

JEC. (2022). Enabling superior storage efficiency for type 4 tanks with fpp dome reinforcements. https://www.jeccomposites.com/news/by-jec/enabling-superior-storage-efficiency-for-type-4-tanks-with-fpp-dome-reinforcements/

Johansson, J., Sundin, E., & Wiktorsson, M. (2019). *Sustainable Manufacturing (pp. 165).*

Johansson, M. (Volvo Principal Energy and Fuel Analyst).

Kaliswal, E, S . Gunnersson. (2024). Lca on hydrogen fuel tanks made of carbon fiber.

Landi, D., & et al. (2020). A methodological approach for the design of composite tanks produced by filament winding. https://www.researchgate.net/publication/339510238_A_Methodological_Approach_for_the_Design_of_Composite_Tanks_Produced_by_Filament_Winding

Le, M. K. (2024). The white gold rush and the pursuit of natural hydrogen. https://www.rystadenergy.com/news/white-gold-rush-pursuit-natural-hydrogen

Liu, A. H. L. B. Y. W. X. M. Y. (2018). Energy consumption modeling of industrial robot based on simulated power data and parameter identification. https://journals.sagepub.com/doi/full/10.1177/1687814018773852

Madhvi, M., & et al. (2009). Design and analysis of filament wound composite pressure vessel with integrated-end domes. https://www.semanticscholar.org/paper/Design-and-Analysis-of-Filament-Wound-Composite-Madhavi/03e35d03cb858a6ef2bb30ac6e42e88d0a062776

Matweb. (2024). Overview of materials for epoxy, molded, glass fiber filler. https://shorturl.at/yMvRT

Meardon, E. (2018). Worldometer. https://www.worldometers.info/world-population/

Mouëllic, M. L., Ventura, A., Heller, K., Loh, A., Roch, R., Spitzbart, J., & Zanotelli, P. (2023). Six strategies for designing sustainable products. https://www.bcg.com/publications/2023/six-strategies-to-lead-product-sustainability-design

Sazedul Islam, M., & et al. (2022). Composite materials: Concept, recent advancements, and applications. https://www.sciencedirect.com/science/article/pii/B978032385155800011X?fr=RR-2&ref=pdf_download&rr=874f926b2d08abd2

Siddiqui, M., & et al. (2023). Analysis of type iv hydrogen pressure vessel with s-glass, carbon fiber t700 and kevlar composite materials. https://www.sciencedirect.com/science/article/pii/S2214785323046989

Systèms, D. (2024). https://www.3ds.com/products/simulia/abaqus

Teter, J. (2023). *Transport*. https://www.iea.org/energy-system/transport

Tooray. (2018). Tooray t700s standard modulas carbon fiber. https://www.toraycma.com/wp-content/uploads/T700S-Technical-Data-Sheet-1.pdf.pdf

Trucks, V. (2024). Resources. https://www.delegia.com/app/Data/ProjectImages/18778/Resources%20station.pdf

Tyson, B. (2020). Reclaimed carbon fibers. https://www.carbonfiberremanufacturing.com/pages/reclaimedCarbonFiber/solution.php

Vujasin, m. (2023). White hydrogen: Sustainable energy from depths of earth. https://balkangreenenergynews.com/white-hydrogen-sustainable-energy-from-depths-of-earth/

Weiszflo, E., & Abbas, M. (2022). *Life Cycle Assessment of Hydrogen Storage Systems for Trucks An assessment of environmental impacts and recycling flows of carbon fiber*. https://hdl.handle.net/20.500.12380/304840

Wright, A. (2022). Reduce, reuse, (repair, refurbish, remanufacture. https://www.linkedin.com/pulse/reduce-reuse-repair-refurbish-remanufacture-recycle-andrew-wright

A
Appendix 1

A.1 Figures and Tables

A.1.1 Requirement Specification

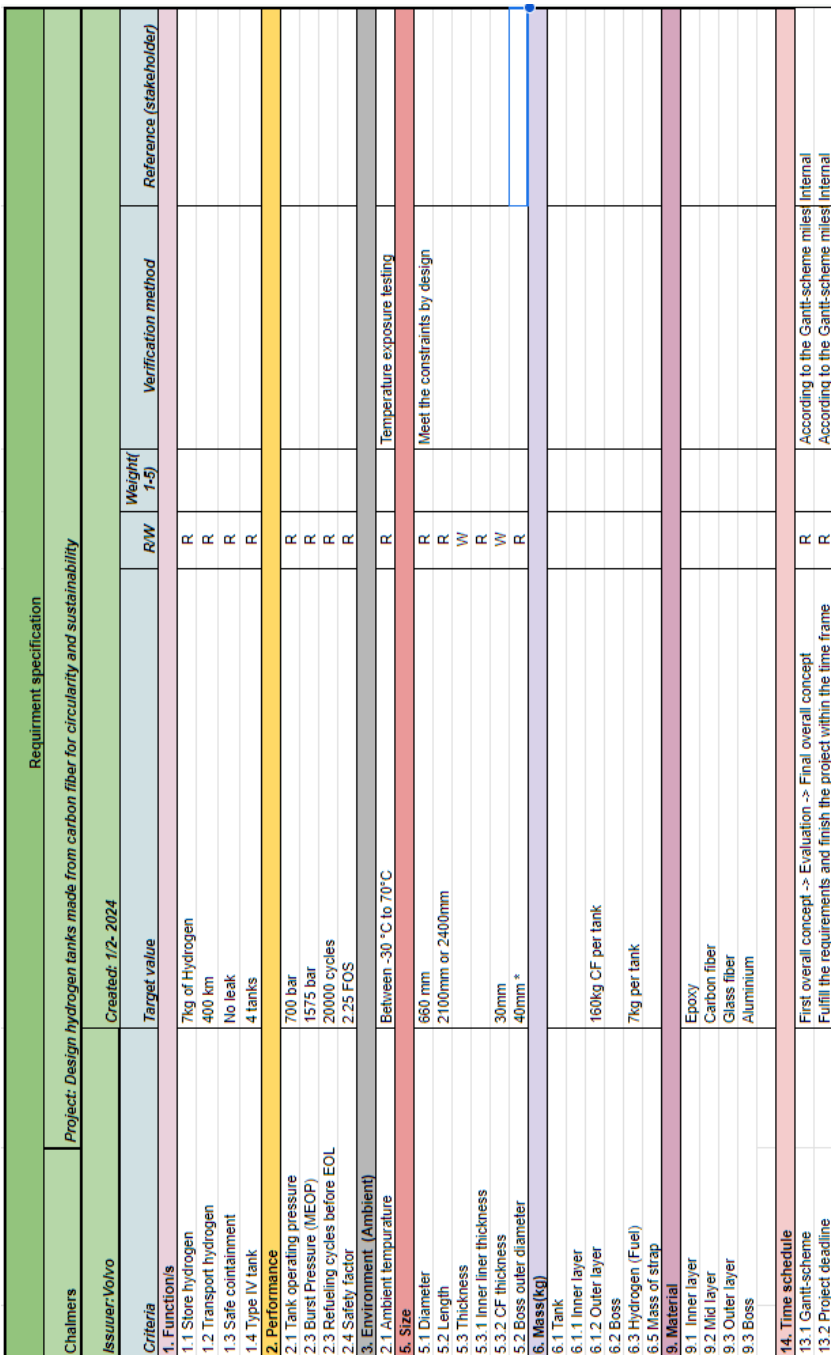

Requirment specification							
Chalmers	Project: Design hydrogen tanks made from carbon fiber for circularity and sustainability						
Issuer:Volvo	Created: 1/2- 2024						
Criteria	Target value	R/W	Weight(1-5)	Verification method	Reference (stakeholder)		
1. Function/s							
1.1 Store hydrogen	7kg of Hydrogen	R					
1.2 Transport hydrogen	400 km	R					
1.3 Safe cointainment	No leak	R					
1.4 Type IV tank	4 tanks	R					
2. Performance							
2.1 Tank operating pressure	700 bar	R					
2.3 Burst Pressure (MEOP)	1575 bar	R					
2.3 Refueling cycles before EOL	20000 cycles	R					
2.4 Safety factor	2.25 FOS	R					
3. Environment (Ambient)							
2.1 Ambient tempuratlure	Between -30 °C to 70°C	R		Temperature exposure testing			
5. Size							
5.1 Diameter	660 mm	R		Meet the constraints by design			
5.2 Length	2100mm or 2400mm	R					
5.3 Thickness		W					
5.3.1 Inner liner thickness		R					
5.3.2 CF thickness	30mm	W					
5.2 Boss outer diameter	40mm *	R					
6. Mass(kg)							
6.1 Tank							
6.1.1 Inner layer							
6.1.2 Outer layer	160kg CF per tank						
6.2 Boss							
6.3 Hydrogen (Fuel)	7kg per tank						
6.5 Mass of strap							
9. Material							
9.1 Inner layer	Epoxy						
9.2 Mid layer	Carbon fiber						
9.3 Outer layer	Glass fiber						
9.3 Boss	Aluminium						
14. Time schedule							
13.1 Gantt-scheme	First overall concept -> Evaluation -> Final overall concept	R		According to the Gantt-scheme miles	Internal		
13.2 Project deadline	Fulfill the requirements and finish the project within the time frame	R		According to the Gantt-scheme miles	Internal		

Figure A.1: Requirement Specification on hydrogen tank

A.1.2 Bill of material

Component	Description	Material	Quantity	Notes
Boss (inlet and reserve tank)	-Act as an interface between valve for and hydrogen storage -Reliable attachment point for valves (1) -Connecting the plastic inner liner and carbon fiber layer to the external metallic valves at the head of the vessels (1) Interface between valve for feeding hydrogen to the cell	Aluminium	2	Provides localized reinforcement for attachment points.
Carbon fiber	-Carbon fiber layer to to withstand the pressure of the compressed hydrogen that is stored as a fuel for the fuel cell -Acts as structural layer with withstand high pressure -It is between the Fiber glass and	CF T700S	1	
Epoxy liner	-To hold the hydrogen within the tank without allowing to permeate through the layers as Hydrogen is a very small molecule -Inner liner in contact with Hygrogen gas	Epoxy or HDP	1	
Fiber glass rienforcement	-Fail safe indicator incase of damage in the outer layer due to sharp contact or drop damage of tank (2) -Fire protection (2)		1	
Dome protector	- Protection for the dome as it is the most sensitive part - Act as protector to the dome when	PPe	1	
Adhesive (boss and liner connection)	- Sealant between epoxy layer, carbon fiber layer and boss (3) -Avoid leakage of hydrogen between the layers (2)		1	
Valves		Metal	1	Material chosen for corrosion resistance and pressure rating

Figure A.2: Bill of material for hydrogen tank, Siddiqui(2023)

A.1.3 Design failure mode effect analysis

Table A.1: DFMEA of the Hydrogen Tank

Item	Potential Failure Mode	Potential Effect(s) of Failure	SEV	Potential Cause(s)/ Mechanism(s) of Failure(s)	OCCUR	DETECT	RPN #
Boss (inlet and reserve tank)	Seal failure between boss, liner and CF	Leakage	7	Material degration(hydrogen exposure, temperature and pressure cycling)	6	4	168
	Structural fail	Rupture or leakage	9	Too high pressure or impact damage	2	2	36
Carbon fiber	Hydrogen Emrittlement	Loss of strength and ductility leading to rupture and crack, release hydrogen	5	Gas slowly diffuse through material(permation)	2	8	80
	Cracking	Fiber tear and explosion	9	Cyclic loading	2	8	144
	Delamination	Seperation of layers and explosion	6	Different properties	2	8	96
Epoxy liner	Degration(permetation) (1)	Loss of mechanical properties(strength and stiffnes) and loss of adhesion between layer	7	Exposure of hydrogen	2	8	112
	Thermal cycling and fattigue (1)	Expoy expand and contract leading to cracks(swelling)	8	Temperature variations under refueling and pressure change induce thermal stress and fattigue	3	8	192

Fiber glass reinforcement	Hydrogen Embrittlement	Loss of strength and ductility leading to rupture and crack, release hydrogen	3	Gas slowly diffuse through material(permation)	1	6	18
	Impact damage	Loss of integrity(cracks, shatters or deformation)	3	Impacts during transportation, installation, operation or flying debris	7	1	21
Dome protector	Impact damage	Loss of integrity(cracks, shatters or deformation)	4	Impacts during transportation, installation, operation or flying debris	7	2	56
	Wear and Tear	Loss function of protecting	4	Friction, stress and fattigue	5	2	40
Valves	Wear and tear	small gaps and allowing hydrogen to leak	7	Cyclic loading and stress(repeated cycles of opening, closing, and pressurization)	8	3	168
	Corrosion	compromising their sealing ability	4	Exposure to moisture and corrosive elements can weaken the valve components	5	3	60
	Debris contamination	can interfere with the proper sealing leading to leak	7	Foreign particles entering the valve	5	3	105

A.1.4 Ply sequence for design 1-8

Table A.2: Whole Ply sequence for design 1 to design 4

Design 1			Design 2			Design 3			Design 4		
Layer type	Angle	Material	Layer type	Angle	Material	Layer type	Angle	Material	Layer type	Angle	Material
Hoop1	85	vCF	Hoop1	85	rCF	Hoop1	85	rCF	Hoop1	85	rCF
Hoop2	-85	vCF	Hoop2	-85	rCF	Hoop2	-85	rCF	Hoop2	-85	rCF
Hoop3	-85	vCF	Hoop3	-85	rCF	Hoop3	-85	rCF	Hoop3	-85	rCF
S1-Interm 1	58	vCF	S1-Interm 1	58	rCF	S1-Interm 1	58	rCF	S1-Interm 1	58	vCF
S1-Interm 2	-58	vCF	S1-Interm 2	-58	rCF	S1-Interm 2	-58	rCF	S1-Interm 2	-58	vCF
S1-Hellical 1	40	vCF	S1-Hellical 1	40	rCF	S1-Hellical 1	40	rCF	S1-Hellical 1	40	vCF
S1-Hellical 2	-40	vCF	S1-Hellical 2	-40	rCF	S1-Hellical 2	-40	rCF	S1-Hellical 2	-40	vCF
S1-Hellical 3	40	vCF	S1-Hellical 3	40	rCF	S1-Hellical 3	40	rCF	S1-Hellical 3	40	vCF
S1-Hellical 4	-40	vCF	S1-Hellical 4	-40	rCF	S1-Hellical 4	-40	rCF	S1-Hellical 4	-40	vCF
S1-Interm 3	58	vCF	S1-Interm 3	58	rCF	S1-Interm 3	58	rCF	S1-Interm 3	58	vCF
S1-Interm 4	-58	vCF	S1-Interm 4	-58	rCF	S1-Interm 4	-58	rCF	S1-Interm 4	-58	vCF
Hoop4	85	vCF	Hoop4	85	rCF	Hoop4	85	rCF	Hoop4	85	rCF
Hoop5	-85	vCF	Hoop5	-85	rCF	Hoop5	-85	rCF	Hoop5	-85	rCF
Hoop6	-85	vCF	Hoop6	-85	rCF	Hoop6	-85	rCF	Hoop6	-85	rCF
S1-Interm 5	58	vCF	S1-Interm 5	58	rCF	S1-Interm 5	58	rCF	S1-Interm 5	58	vCF
S1-Interm 6	-58	vCF	S1-Interm 6	-58	rCF	S1-Interm 6	-58	rCF	S1-Interm 6	-58	vCF
S1-Hellical 5	38.5	vCF	S1-Hellical 5	38.5	rCF	S1-Hellical 5	38.5	rCF	S1-Hellical 5	38.5	vCF
S1-Hellical 6	-38.5	vCF	S1-Hellical 6	-38.5	rCF	S1-Hellical 6	-38.5	rCF	S1-Hellical 6	-38.5	vCF
S1-Hellical 7	38.5	vCF	S1-Hellical 7	38.5	rCF	S1-Hellical 7	38.5	rCF	S1-Hellical 7	38.5	vCF
S1-Hellical 8	-38.5	vCF	S1-Hellical 8	-38.5	rCF	S1-Hellical 8	-38.5	rCF	S1-Hellical 8	-38.5	vCF
S1-Interm 7	58	vCF	S1-Interm 7	58	rCF	S1-Interm 7	58	rCF	S1-Interm 7	58	vCF
S1-Interm 8	-58	vCF	S1-Interm 8	-58	rCF	S1-Interm 8	-58	rCF	S1-Interm 8	-58	vCF
Hoop7	85	vCF	Hoop7	85	rCF	Hoop7	85	rCF	Hoop7	85	rCF
Hoop8	-85	vCF	Hoop8	-85	rCF	Hoop8	-85	rCF	Hoop8	-85	rCF
Hoop9	-85	vCF	Hoop9	-85	rCF	Hoop9	-85	rCF	Hoop9	-85	rCF
S1-Interm 9	58	vCF	S1-Interm 9	58	rCF	S1-Interm 9	58	rCF	S1-Interm 9	58	vCF
S1-Interm 10	-58	vCF	S1-Interm 10	-58	rCF	S1-Interm 10	-58	rCF	S1-Interm 10	-58	vCF
S1-Hellical 9	37	vCF	S1-Hellical 9	37	rCF	S1-Hellical 9	37	rCF	S1-Hellical 9	37	vCF
S1-Hellical 10	-37	vCF	S1-Hellical 10	-37	rCF	S1-Hellical 10	-37	rCF	S1-Hellical 10	-37	vCF
S1-Hellical 11	37	vCF	S1-Hellical 11	37	rCF	S1-Hellical 11	37	rCF	S1-Hellical 11	37	vCF
S1-Hellical 12	-37	vCF	S1-Hellical 12	-37	rCF	S1-Hellical 12	-37	rCF	S1-Hellical 12	-37	vCF
S1-Interm 11	58	vCF	S1-Interm 11	58	rCF	S1-Interm 11	58	rCF	S1-Interm 11	58	vCF
S1-Interm 12	-58	vCF	S1-Interm 12	-58	rCF	S1-Interm 12	-58	rCF	S1-Interm 12	-58	vCF
Hoop10	85	vCF	Hoop10	85	rCF	Hoop10	85	rCF	Hoop10	85	rCF
Hoop11	-85	vCF	Hoop11	-85	rCF	Hoop11	-85	rCF	Hoop11	-85	rCF
Hoop12	-85	vCF	Hoop12	-85	rCF	Hoop12	-85	rCF	Hoop12	-85	rCF
S1-Interm 13	58	vCF	S1-Interm 13	58	rCF	S1-Interm 13	58	rCF	S1-Interm 13	58	vCF
S1-Interm 14	-58	vCF	S1-Interm 14	-58	rCF	S1-Interm 14	-58	rCF	S1-Interm 14	-58	vCF
S1-Hellical 13	35	vCF	S1-Hellical 13	35	rCF	S1-Hellical 13	35	rCF	S1-Hellical 13	35	vCF
S1-Hellical 14	-35	vCF	S1-Hellical 14	-35	rCF	S1-Hellical 14	-35	rCF	S1-Hellical 14	-35	vCF
S1-Hellical 15	35	vCF	S1-Hellical 15	35	rCF	S1-Hellical 15	35	rCF	S1-Hellical 15	35	vCF
S1-Hellical 16	-35	vCF	S1-Hellical 16	-35	rCF	S1-Hellical 16	-35	rCF	S1-Hellical 16	-35	vCF
S1-Interm 15	58	vCF	S1-Interm 15	58	rCF	S1-Interm 15	58	rCF	S1-Interm 15	58	vCF
S1-Interm 16	-58	vCF	S1-Interm 16	-58	rCF	S1-Interm 16	-58	rCF	S1-Interm 16	-58	vCF
Hoop13	85	vCF	Hoop13	85	rCF	Hoop13	85	rCF	Hoop13	85	rCF
Hoop14	-85	vCF	Hoop14	-85	rCF	Hoop14	-85	rCF	Hoop14	-85	rCF
S2-Inter 1	58	vCF	S2-Inter 1	58	rCF	S2-Inter 1	58	rCF	S2-Inter 1	58	vCF
S2-Inter 2	-58	vCF	S2-Inter 2	-58	rCF	S2-Inter 2	-58	rCF	S2-Inter 2	-58	vCF
S2-Hellical 1	33	vCF	S2-Hellical 1	33	rCF	S2-Hellical 1	33	rCF	S2-Hellical 1	33	vCF
S2-Hellical 2	-33	vCF	S2-Hellical 2	-33	rCF	S2-Hellical 2	-33	rCF	S2-Hellical 2	-33	vCF
S2-Hellical 3	32.5	vCF	S2-Hellical 3	32.5	rCF	S2-Hellical 3	32.5	rCF	S2-Hellical 3	32.5	vCF
S2-Hellical 4	-32.5	vCF	S2-Hellical 4	-32.5	rCF	S2-Hellical 4	-32.5	rCF	S2-Hellical 4	-32.5	vCF
S2-Inter 3	58	vCF	S2-Inter 3	58	rCF	S2-Inter 3	58	rCF	S2-Inter 3	58	vCF
S2-Inter 4	-58	vCF	S2-Inter 4	-58	rCF	S2-Inter 4	-58	rCF	S2-Inter 4	-58	vCF
Hoop15	85	vCF	Hoop15	85	rCF	Hoop15	85	rCF	Hoop15	85	rCF
Hoop16	-85	vCF	Hoop16	-85	rCF	Hoop16	-85	rCF	Hoop16	-85	rCF
S2-Inter 5	58	vCF	S2-Inter 5	58	rCF	S2-Inter 5	58	rCF	S2-Inter 5	58	vCF
S2-Inter 6	-58	vCF	S2-Inter 6	-58	rCF	S2-Inter 6	-58	rCF	S2-Inter 6	-58	vCF
S2-Hellical 5	27	vCF	S2-Hellical 5	27	rCF	S2-Hellical 5	27	rCF	S2-Hellical 5	27	vCF
S2-Hellical 6	-27	vCF	S2-Hellical 6	-27	rCF	S2-Hellical 6	-27	rCF	S2-Hellical 6	-27	vCF
S2-Hellical 7	27	vCF	S2-Hellical 7	27	rCF	S2-Hellical 7	27	rCF	S2-Hellical 7	27	vCF
S2-Hellical 8	-27	vCF	S2-Hellical 8	-27	rCF	S2-Hellical 8	-27	rCF	S2-Hellical 8	-27	vCF
S2-Inter 7	58	vCF	S2-Inter 7	58	rCF	S2-Inter 7	58	rCF	S2-Inter 7	58	vCF
S2-Inter 8	-58	vCF	S2-Inter 8	-58	rCF	S2-Inter 8	-58	rCF	S2-Inter 8	-58	vCF
Hoop17	85	vCF	Hoop17	85	rCF	Hoop17	85	rCF	Hoop17	85	rCF
Hoop18	-85	vCF	Hoop18	-85	rCF	Hoop18	-85	rCF	Hoop18	-85	rCF
S2-Inter 9	58	vCF	S2-Inter 9	58	rCF	S2-Inter 9	58	rCF	S2-Inter 9	58	vCF
S2-Inter 10	-58	vCF	S2-Inter 10	-58	rCF	S2-Inter 10	-58	rCF	S2-Inter 10	-58	vCF
S2-Hellical 9	22	vCF	S2-Hellical 9	22	rCF	S2-Hellical 9	22	rCF	S2-Hellical 9	22	vCF
S2-Hellical 10	-22	vCF	S2-Hellical 10	-22	rCF	S2-Hellical 10	-22	rCF	S2-Hellical 10	-22	vCF
S2-Hellical 11	22	vCF	S2-Hellical 11	22	rCF	S2-Hellical 11	22	rCF	S2-Hellical 11	22	vCF
S2-Hellical 12	-22	vCF	S2-Hellical 12	-22	rCF	S2-Hellical 12	-22	rCF	S2-Hellical 12	-22	vCF
S2-Inter 11	58	vCF	S2-Inter 11	58	rCF	S2-Inter 11	58	rCF	S2-Inter 11	58	vCF
S2-Inter 12	-58	vCF	S2-Inter 12	-58	rCF	S2-Inter 12	-58	rCF	S2-Inter 12	-58	vCF
Hoop19	85	vCF	Hoop19	85	rCF	Hoop19	85	rCF	Hoop19	85	rCF
Hoop20	-85	vCF	Hoop20	-85	rCF	Hoop20	-85	rCF	Hoop20	-85	rCF
S3-Inter 13	58	vCF	S3-Inter 13	58	rCF	S3-Inter 13	58	rCF	S3-Inter 13	58	vCF
S3-Inter 14	-58	vCF	S3-Inter 14	-58	rCF	S3-Inter 14	-58	rCF	S3-Inter 14	-58	vCF
S3-Hellical 13	16	vCF	S3-Hellical 13	16	rCF	S3-Hellical 13	16	rCF	S3-Hellical 13	16	vCF
S3-Hellical 14	-16	vCF	S3-Hellical 14	-16	rCF	S3-Hellical 14	-16	rCF	S3-Hellical 14	-16	vCF
S3-Hellical 15	16	vCF	S3-Hellical 15	16	rCF	S3-Hellical 15	16	rCF	S3-Hellical 15	16	vCF
S3-Hellical 16	-16	vCF	S3-Hellical 16	-16	rCF	S3-Hellical 16	-16	rCF	S3-Hellical 16	-16	vCF
S3-Inter 15	58	vCF	S3-Inter 15	58	rCF	S3-Inter 15	58	rCF	S3-Inter 15	58	vCF
S3-Inter 16	-58	vCF	S3-Inter 16	-58	rCF	S3-Inter 16	-58	rCF	S3-Inter 16	-58	vCF
Hoop21	85	vCF	Hoop21	85	rCF	Hoop21	85	rCF	Hoop21	85	rCF
S3-Inter 17	58	vCF	S3-Inter 17	58	rCF	S3-Inter 17	58	rCF	S3-Inter 17	58	vCF
S3-Inter 18	-58	vCF	S3-Inter 18	-58	rCF	S3-Inter 18	-58	rCF	S3-Inter 18	-58	vCF
S3-Hellical 17	13	vCF	S3-Hellical 17	13	rCF	S3-Hellical 17	13	rCF	S3-Hellical 17	13	vCF
S3-Hellical 18	-13	vCF	S3-Hellical 18	-13	rCF	S3-Hellical 18	-13	rCF	S3-Hellical 18	-13	vCF
S3-Hellical 19	13	vCF	S3-Hellical 19	13	rCF	S3-Hellical 19	13	rCF	S3-Hellical 19	13	vCF
S3-Hellical 20	-13	vCF	S3-Hellical 20	-13	rCF	S3-Hellical 20	-13	rCF	S3-Hellical 20	-13	vCF
S3-Inter 19	58	vCF	S3-Inter 19	58	rCF	S3-Inter 19	58	rCF	S3-Inter 19	58	vCF
S3-Inter 20	-58	vCF	S3-Inter 20	-58	rCF	S3-Inter 20	-58	rCF	S3-Inter 20	-58	vCF
Hoop22	90	vCF	Hoop22	90	rCF	Hoop22	90	rCF	Hoop22	90	rCF
S4-Inter 21	58	vCF	S4-Inter 21	58	rCF	S4-Inter 21	58	rCF	S4-Inter 21	58	vCF
S4-Inter 22	-58	vCF	S4-Inter 22	-58	rCF	S4-Inter 22	-58	rCF	S4-Inter 22	-58	vCF
S4-Hellical 21	30	vCF	S4-Hellical 21	30	rCF	S4-Hellical 21	30	rCF	S4-Hellical 21	30	vCF
S4-Hellical 22	-30	vCF	S4-Hellical 22	-30	rCF	S4-Hellical 22	-30	rCF	S4-Hellical 22	-30	vCF
S4-Hellical 23	30	vCF	S4-Hellical 23	30	rCF	S4-Hellical 23	30	rCF	S4-Hellical 23	30	vCF
S4-Hellical 24	-30	vCF	S4-Hellical 24	-30	rCF	S4-Hellical 24	-30	rCF	S4-Hellical 24	-30	vCF
S4-Inter 23	59	vCF	S4-Inter 23	59	rCF	S4-Inter 23	59	rCF	S4-Inter 23	59	vCF
S4-Inter 24	-59	vCF	S4-Inter 24	-59	rCF	S4-Inter 24	-59	rCF	S4-Inter 24	-59	vCF
Hoop23	90	vCF	Hoop23	90	rCF	Hoop23	90	rCF	Hoop23	90	rCF
S4-Inter 25	58	vCF	S4-Inter 25	58	rCF	S4-Inter 25	58	rCF	S4-Inter 25	58	vCF
S4-Inter 26	-58	vCF	S4-Inter 26	-58	rCF	S4-Inter 26	-58	rCF	S4-Inter 26	-58	vCF
S4-Inter 27	58	vCF	S4-Inter 27	58	rCF	S4-Inter 27	58	rCF	S4-Inter 27	58	vCF
S4-Inter 28	-58	vCF	S4-Inter 28	-58	rCF	S4-Inter 28	-58	rCF	S4-Inter 28	-58	vCF
S4-Inter 29	58	vCF	S4-Inter 29	58	rCF	S4-Inter 29	58	rCF	S4-Inter 29	58	vCF
S4-Inter 30	-58	vCF	S4-Inter 30	-58	rCF	S4-Inter 30	-58	rCF	S4-Inter 30	-58	vCF
S4-Hellical 25	30	vCF	S4-Hellical 25	30	rCF	S4-Hellical 25	30	rCF	S4-Hellical 25	30	vCF
S4-Hellical 26	-30	vCF	S4-Hellical 26	-30	rCF	S4-Hellical 26	-30	rCF	S4-Hellical 26	-30	vCF
S4-Inter 31	58	vCF	S4-Inter 31	58	rCF	S4-Inter 31	58	rCF	S4-Inter 31	58	vCF
S4-Inter 32	-58	vCF	S4-Inter 32	-58	rCF	S4-Inter 32	-58	rCF	S4-Inter 32	-58	vCF
S4-Inter 33	58	vCF	S4-Inter 33	58	rCF	S4-Inter 33	58	rCF	S4-Inter 33	58	vCF
S4-Inter 34	-58	vCF	S4-Inter 34	-58	rCF	S4-Inter 34	-58	rCF	S4-Inter 34	-58	vCF
			S4-Inter 36	58	rCF	S4-Inter 36	58	rCF			
			S4-Inter 37	-58	rCF	S4-Inter 37	-58	rCF			

A.1.5 Ply sequence for design 1-8

Table A.3: Whole Ply sequence for design 5 to design 8

Design 5			Design 6			Design 7			Design 8		
Layer type	Angle	Material	Layer type	Angle	Material	Layer type	Angle	Material	Layer type	Angle	Material
Doily 1	8	vCF	Doily 1	8	rCF	Hoop1	85	vCF	Hoop1	85	rCF
Doily 2	8	vCF	Doily 2	8	rCF	Hoop2	-85	vCF	Hoop2	-85	rCF
Doily 3	7	vCF	Doily 3	7	rCF	Hoop3	-85	vCF	Hoop3	-85	rCF
Doily 4	6	vCF	Doily 4	6	rCF	S1-Interm 1	58	vCF	S1-Interm 1	58	rCF
Doily 5	6	vCF	Doily 5	6	rCF	S1-Interm 2	-58	vCF	S1-Interm 2	-58	rCF
Doily 6	6	vCF	Doily 6	6	rCF	S1-Helical 1	40	vCF	S1-Helical 1	40	rCF
Doily 7	5	vCF	Doily 7	5	rCF	S1-Helical 2	-40	vCF	S1-Helical 2	-40	rCF
Doily 8	5	vCF	Doily 8	5	rCF	S1-Helical 3	40	vCF	S1-Helical 3	40	rCF
Doily 9	5	vCF	Doily 9	5	rCF	S1-Helical 4	-40	vCF	S1-Helical 4	-40	rCF
Doily 10	4	vCF	Doily 10	4	rCF	S1-Interm 3	58	vCF	S1-Interm 3	58	rCF
Doily 11	3	vCF	Doily 11	3	rCF	S1-Interm 4	-58	vCF	S1-Interm 4	-58	rCF
Doily 12	3	vCF	Doily 12	3	rCF	Hoop4	85	vCF	Hoop4	85	rCF
Doily 13	3	vCF	Doily 13	3	rCF	Hoop5	-85	vCF	Hoop5	-85	rCF
Doily 14	2	vCF	Doily 14	2	rCF	Hoop6	-85	vCF	Hoop6	-85	rCF
Doily 15	1	vCF	Doily 15	1	rCF	S1-Interm 5	58	vCF	S1-Interm 5	58	rCF
Doily 16	1	vCF	Doily 16	1	rCF	S1-Interm 6	-58	vCF	S1-Interm 6	-58	rCF
Doily 17	0	vCF	Doily 17	0	rCF	S1-Helical 5	38.5	vCF	S1-Helical 5	38.5	rCF
Doily 18	0	vCF	Doily 18	0	rCF	S1-Helical 6	-38.5	vCF	S1-Helical 6	-38.5	rCF
Doily 19	0	vCF	Doily 19	0	rCF	S1-Helical 7	38.5	vCF	S1-Helical 7	38.5	rCF
Doily 20	0	vCF	Doily 20	0	rCF	S1-Helical 8	-38.5	vCF	S1-Helical 8	-38.5	rCF
Doily 21	0	vCF	Doily 21	0	rCF	S1-Interm 7	58	vCF	S1-Interm 7	58	rCF
Hoop1	85	vCF	Hoop1	85	vCF	S1-Interm 8	-58	vCF	S1-Interm 8	-58	rCF
Hoop2	-85	vCF	Hoop2	-85	vCF	Hoop7	85	vCF	Hoop7	85	rCF
Hoop3	-85	vCF	Hoop3	-85	vCF	Hoop8	-85	vCF	Hoop8	-85	rCF
S1-Interm 1	59	vCF	S1-Interm 1	59	vCF	Hoop9	-85	vCF	Hoop9	-85	rCF
S1-Interm 2	-59	vCF	S1-Interm 2	-59	vCF	S1-Interm 9	58	vCF	S1-Interm 9	58	rCF
S1-Helical 1	40	vCF	S1-Helical 1	40	vCF	S1-Interm 10	-58	vCF	S1-Interm 10	-58	rCF
S1-Helical 2	-40	vCF	S1-Helical 2	-40	vCF	S1-Helical 9	37	vCF	S1-Helical 9	37	rCF
S1-Helical 3	38.5	vCF	S1-Helical 3	38.5	vCF	S1-Helical 10	-37	vCF	S1-Helical 10	-37	rCF
S1-Helical 4	-38.5	vCF	S1-Helical 4	-38.5	vCF	S1-Helical 11	37	vCF	S1-Helical 11	37	rCF
S1-Interm 3	59	vCF	S1-Interm 3	59	vCF	S1-Helical 12	-37	vCF	S1-Helical 12	-37	rCF
S1-Interm 4	-59	vCF	S1-Interm 4	-59	vCF	S1-Interm 11	58	vCF	S1-Interm 11	58	rCF
Hoop4	85	vCF	Hoop4	85	vCF	S1-Interm 12	-58	vCF	S1-Interm 12	-58	rCF
Hoop5	-85	vCF	Hoop5	-85	vCF	Hoop10	85	vCF	Hoop10	85	rCF
Hoop6	-85	vCF	Hoop6	-85	vCF	Hoop11	-85	vCF	Hoop11	-85	rCF
S1-Interm 5	59	vCF	S1-Interm 5	59	vCF	Hoop12	-85	vCF	Hoop12	-85	rCF
S1-Interm 6	-59	vCF	S1-Interm 6	-59	vCF	S1-Interm 13	58	vCF	S1-Interm 13	58	rCF
S1-Helical 5	37.5	vCF	S1-Helical 5	37.5	vCF	S1-Interm 14	-58	vCF	S1-Interm 14	-58	rCF
S1-Helical 6	-37.5	vCF	S1-Helical 6	-37.5	vCF	S1-Helical 13	35	vCF	S1-Helical 13	35	rCF
S1-Helical 7	36	vCF	S1-Helical 7	36	vCF	S1-Helical 14	-35	vCF	S1-Helical 14	-35	rCF
S1-Helical 8	-36	vCF	S1-Helical 8	-36	vCF	S1-Helical 15	35	vCF	S1-Helical 15	35	rCF
S1-Interm 7	59	vCF	S1-Interm 7	59	vCF	S1-Helical 16	-35	vCF	S1-Helical 16	-35	rCF
S1-Interm 8	-59	vCF	S1-Interm 8	-59	vCF	S1-Interm 15	58	vCF	S1-Interm 15	58	rCF
Hoop7	85	vCF	Hoop7	85	vCF	S1-Interm 16	-58	vCF	S1-Interm 16	-58	rCF
Hoop8	-85	vCF	Hoop8	-85	vCF	Hoop13	85	vCF	Hoop13	85	rCF
Hoop9	-85	vCF	Hoop9	-85	vCF	Hoop14	-85	vCF	Hoop14	-85	rCF
S1-Interm 9	59	vCF	S1-Interm 9	59	vCF	S2-Inter 1	58	vCF	S2-Inter 1	58	rCF
S1-Interm 10	-59	vCF	S1-Interm 10	-59	vCF	S2-Inter 2	-58	vCF	S2-Inter 2	-58	rCF
S1-Helical 9	35	vCF	S1-Helical 9	35	vCF	S2-Helical 1	33	vCF	S2-Helical 1	33	rCF
S1-Helical 10	-35	vCF	S1-Helical 10	-35	vCF	S2-Helical 2	-33	vCF	S2-Helical 2	-33	rCF
S1-Helical 11	34	vCF	S1-Helical 11	34	vCF	S2-Helical 3	32.5	vCF	S2-Helical 3	32.5	rCF
S1-Helical 12	-34	vCF	S1-Helical 12	-34	vCF	S2-Helical 4	-32.5	vCF	S2-Helical 4	-32.5	rCF
S1-Interm 11	59	vCF	S1-Interm 11	59	vCF	S2-Inter 3	58	vCF	S2-Inter 3	58	rCF
S1-Interm 12	-59	vCF	S1-Interm 12	-59	vCF	S2-Inter 4	-58	vCF	S2-Inter 4	-58	rCF
Hoop10	85	vCF	Hoop10	85	vCF	Hoop15	85	vCF	Hoop15	85	rCF
Hoop11	-85	vCF	Hoop11	-85	vCF	Hoop16	-85	vCF	Hoop16	-85	rCF
Hoop12	-85	vCF	Hoop12	-85	vCF	S2-Inter 5	58	vCF	S2-Inter 5	58	rCF
S1-Interm 13	58	vCF	S1-Interm 13	58	vCF	S2-Inter 6	-58	vCF	S2-Inter 6	-58	rCF
S1-Interm 14	-58	vCF	S1-Interm 14	-58	vCF	S2-Helical 5	27	vCF	S2-Helical 5	27	rCF
S1-Helical 13	33	vCF	S1-Helical 13	33	vCF	S2-Helical 6	-27	vCF	S2-Helical 6	-27	rCF
S1-Helical 14	-33	vCF	S1-Helical 14	-33	vCF	S2-Helical 7	27	vCF	S2-Helical 7	27	rCF
S1-Helical 15	32	vCF	S1-Helical 15	32	vCF	S2-Helical 8	-27	vCF	S2-Helical 8	-27	rCF
S1-Helical 16	-32	vCF	S1-Helical 16	-32	vCF	S2-Inter 7	58	vCF	S2-Inter 7	58	rCF
S1-Interm 15	58	vCF	S1-Interm 15	58	vCF	S2-Inter 8	-58	vCF	S2-Inter 8	-58	rCF
S1-Interm 16	-58	vCF	S1-Interm 16	-58	vCF	Hoop17	85	vCF	Hoop17	85	rCF
Hoop13	85	vCF	Hoop13	85	vCF	Hoop18	-85	vCF	Hoop18	-85	rCF
Hoop14	-85	vCF	Hoop14	-85	vCF	S2-Inter 9	58	vCF	S2-Inter 9	58	rCF
S2-Inter 1	58	vCF	S2-Inter 1	58	vCF	S2-Inter 10	-58	vCF	S2-Inter 10	-58	rCF
S2-Inter 2	-58	vCF	S2-Inter 2	-58	vCF	S2-Helical 9	22	vCF	S2-Helical 9	22	rCF
S2-Helical 1	32	vCF	S2-Helical 1	32	vCF	S2-Helical 10	-22	vCF	S2-Helical 10	-22	rCF
S2-Helical 2	-32	vCF	S2-Helical 2	-32	vCF	S2-Helical 11	22	vCF	S2-Helical 11	22	rCF
S2-Helical 3	30	vCF	S2-Helical 3	30	vCF	S2-Helical 12	-22	vCF	S2-Helical 12	-22	rCF
S2-Helical 4	-30	vCF	S2-Helical 4	-30	vCF	S2-Inter 11	58	vCF	S2-Inter 11	58	rCF
S2-Inter 3	58	vCF	S2-Inter 3	58	vCF	S2-Inter 12	-58	vCF	S2-Inter 12	-58	rCF
S2-Inter 4	-58	vCF	S2-Inter 4	-58	vCF	Hoop19	85	vCF	Hoop19	85	rCF
Hoop15	85	vCF	Hoop15	85	vCF	Hoop20	-85	vCF	Hoop20	-85	rCF
Hoop16	-85	vCF	Hoop16	-85	vCF	S3-Inter 13	58	vCF	S3-Inter 13	58	rCF
S2-Inter 5	57	vCF	S2-Inter 5	57	vCF	S3-Inter 14	-58	vCF	S3-Inter 14	-58	rCF
S2-Inter 6	-57	vCF	S2-Inter 6	-57	vCF	S3-Helical 13	16	vCF	S3-Helical 13	16	rCF
S2-Helical 5	25	vCF	S2-Helical 5	25	vCF	S3-Helical 14	-16	vCF	S3-Helical 14	-16	rCF
S2-Helical 6	-25	vCF	S2-Helical 6	-25	vCF	S3-Helical 15	16	vCF	S3-Helical 15	16	rCF
S2-Helical 7	25	vCF	S2-Helical 7	25	vCF	S3-Helical 16	-16	vCF	S3-Helical 16	-16	rCF
S2-Helical 8	-25	vCF	S2-Helical 8	-25	vCF	S3-Inter 15	58	vCF	S3-Inter 15	58	rCF
S2-Inter 7	57	vCF	S2-Inter 7	57	vCF	S3-Inter 16	-58	vCF	S3-Inter 16	-58	rCF
S2-Inter 8	-57	vCF	S2-Inter 8	-57	vCF	Hoop21	85	vCF	Hoop21	85	rCF
Hoop17	85	vCF	Hoop17	85	vCF	S3-Inter 17	58	vCF	S3-Inter 17	58	rCF
Hoop18	-85	vCF	Hoop18	-85	vCF	S3-Inter 18	-58	vCF	S3-Inter 18	-58	rCF
S2-Inter 9	56	vCF	S2-Inter 9	56	vCF	S3-Helical 17	13	vCF	S3-Helical 17	13	rCF
S2-Inter 10	-56	vCF	S2-Inter 10	-56	vCF	S3-Helical 18	-13	vCF	S3-Helical 18	-13	rCF
S2-Helical 9	20	vCF	S2-Helical 9	20	vCF	S3-Helical 19	13	vCF	S3-Helical 19	13	rCF
S2-Helical 10	-20	vCF	S2-Helical 10	-20	vCF	S3-Helical 20	-13	vCF	S3-Helical 20	-13	rCF
S2-Helical 11	20	vCF	S2-Helical 11	20	vCF	S3-Inter 19	58	vCF	S3-Inter 19	58	rCF
S2-Helical 12	-20	vCF	S2-Helical 12	-20	vCF	S3-Inter 20	-58	vCF	S3-Inter 20	-58	rCF
S2-Inter 11	56	vCF	S2-Inter 11	56	vCF	S4-Inter 21	58	vCF	S4-Inter 21	58	rCF
S2-Inter 12	-56	vCF	S2-Inter 12	-56	vCF	S4-Inter 22	-58	vCF	S4-Inter 22	-58	rCF
Hoop19	85	vCF	Hoop19	85	vCF	S4-Helical 21	30	vCF	S4-Helical 21	30	rCF
Hoop20	-85	vCF	Hoop20	-85	vCF	S4-Helical 22	-30	vCF	S4-Helical 22	-30	rCF
S3-Inter 13	55	vCF	S3-Inter 13	55	vCF	S4-Helical 23	30	vCF	S4-Helical 23	30	rCF
S3-Inter 14	-55	vCF	S3-Inter 14	-55	vCF	S4-Helical 24	-30	vCF	S4-Helical 24	-30	rCF
S3-Helical 13	16	vCF	S3-Helical 13	16	vCF	S4-Inter 23	59	vCF	S4-Inter 23	59	rCF
S3-Helical 14	-16	vCF	S3-Helical 14	-16	vCF	S4-Inter 24	-59	vCF	S4-Inter 24	-59	rCF
S3-Inter 15	55	vCF	S3-Inter 15	55	vCF	S4-Inter 25	58	vCF	S4-Inter 25	58	rCF
S3-Inter 16	-55	vCF	S3-Inter 16	-55	vCF	S4-Inter 26	-58	vCF	S4-Inter 26	-58	rCF
Hoop21	85	vCF	Hoop21	85	vCF	S4-Inter 27	58	vCF	S4-Inter 27	58	rCF
Hoop22	-85	vCF	Hoop22	-85	vCF	S4-Inter 28	-58	vCF	S4-Inter 28	-58	rCF
S3-Inter 17	53	vCF	S3-Inter 17	53	vCF	S4-Inter 29	58	vCF	S4-Inter 29	58	rCF
S3-Inter 18	-53	vCF	S3-Inter 18	-53	vCF	S4-Inter 30	-58	vCF	S4-Inter 30	-58	rCF
S3-Helical 17	13	vCF	S3-Helical 17	13	vCF						
S3-Helical 18	-13	vCF	S3-Helical 18	-13	vCF						
S3-Inter 19	53	vCF	S3-Inter 19	53	vCF						
S3-Inter 20	-53	vCF	S3-Inter 20	-53	vCF						
Hoop23	90	vCF	Hoop23	90	vCF						
Hoop24	90	vCF	Hoop24	90	vCF						
S4-Inter 21	58	vCF	S4-Inter 21	58	vCF						
S4-Inter 22	-58	vCF	S4-Inter 22	-58	vCF						
S4-Helical 21	30	vCF	S4-Helical 21	30	vCF						
S4-Helical 22	-30	vCF	S4-Helical 22	-30	vCF						
S4-Inter 23	59	vCF	S4-Inter 23	59	vCF						
S4-Inter 24	-59	vCF	S4-Inter 24	-59	vCF						
Hoop25	90	vCF	Hoop25	90	vCF						
S4-Inter 25	58	vCF	S4-Inter 25	58	vCF						
S4-Inter 26	-58	vCF	S4-Inter 26	-58	vCF						
S4-Inter 27	58	vCF	S4-Inter 27	58	vCF						
S4-Inter 28	-58	vCF	S4-Inter 28	-58	vCF						

A.2 CF Layer thickness calculator

,

```
import math
import matplotlib.pyplot as plt

def calculate_ta(P, R, a, siga):  # Helical
    ta = (P*R)/(2*siga*math.cos(math.radians(a))**2)
    return ta

def calculate_tf(P, R, a, sigf):  # Hoop
    tf = ((P*R)*(2-math.tan(math.radians(a))**2))/(2*sigf)
    return tf

# Define variables
P = 70  # pressure in (MPa)
R = 330  # radius of the tank (mm)
siga = 1271  # allowable stress for helical layer in MPa
sigf = 1271  # allowable stress for hoop layer in MPa

# Create lists to store results
angles = []
ta_values = []
tf_values = []

# Calculate values for each angle from 0 to 90
for a in range(0, 910, 1):
    angle = a / 10.0  # Convert to degrees
    ta_value = calculate_ta(P, R, angle, siga)  # Helical
    tf_value = calculate_tf(P, R, angle, sigf)  # Hoop

    # Only if the calculated values are positive
    if ta_value > 0 and tf_value > 0:
        angles.append(angle)
        ta_values.append(ta_value)
        tf_values.append(tf_value)

# Plot scatter plot
plt.figure(figsize=(10, 6))
plt.scatter(angles, ta_values, label='Helical layer thickness')
plt.scatter(angles, tf_values, label='Hoop layer thickness')
plt.xlabel('Angle (degrees)')
plt.ylabel('Thickness (mm)')
plt.title('Thickness vs. Angle')
plt.legend()
plt.grid(True)
plt.show()
# Print all values for each angle from 0 to 90
print("Angle(deg)\tHelical thickness(mm)\tHoop thickness(mm)")
for angle,ta_value,tf_value in zip(angles,ta_values,tf_values):
    print(f"{angle:.1f}\t\t\t{ta_value:.3f}\t\t\t{tf_value:.3f}")
```

A.3 Mass calculator

,

```
1
2  import math
3
4  def calculate_CFmass(tank_volume, CFdensity):
5      CFmass = (((tank_volume*4)-22905512)*0.6) * CFdensity
6      return CFmass
7
8  def calculate_mass(CFmass,tank_volume, Edensity):
9      mass = (CFmass) + (((tank_volume*4))*0.4 * Edensity)
10     return mass
11
12 def calculate_Rmass(CFmass,mass):
13     Rmass = mass - CFmass
14     return Rmass
15 #Data
16 CFdensity= 0.0000018 #(kg/mm3)
17 Edensity= 0.00000173 #(kg/mm3)
18
19
20 tank_volume = float(input("Enter␣the␣volume␣of␣the␣whole␣tank:␣"))
21
22 CFmass = calculate_CFmass(tank_volume, CFdensity)
23 mass = calculate_mass(CFmass, tank_volume, Edensity)
24 Rmass = calculate_Rmass (CFmass,mass)
25
26 print("The␣mass␣of␣the␣material␣is:", mass)
27 print("The␣mass␣of␣the␣CF␣part␣is:", CFmass)
28 print("The␣mass␣of␣the␣Resin␣part␣is:", Rmass)
```

A.4 Dome profile generator

,

```

import math
import matplotlib.pyplot as plt
from scipy.integrate import quad

def calculate_S(k, Y, Q, r):
    x = Y**2 * ((Y**2) + (r * Q**2))**2
    y = ((1 + r)**2) * Q**6
    m = (k - 1 + Y**2) / (k - 1 + Q**2)
    b = math.sqrt((m**(k + 1) * y) - x)
    a = Y * ((Y**2) + r * Q**2)
    S = a / b
    return S

def integrand(p, k_value, Q_value, r_value):
    Y_value = p / c
    return calculate_S(k_value, Y_value, Q_value, r_value)

# Given values
c = 40   # Example value for c
R = 330  # Example value for R

# Calculate 'Q' based on 'R' and 'c'
Q_value = R / c

# Given value for 'r'
r_value = 0

# List of k values to plot
k_values = [0.088]

# Plotting the graph for each value of k
for k_value in k_values:
    Z_values = []
    for p in range(40, 330):
        Z,_=quad(integrand,40,p,args=(k_value,Q_value,r_value))
        Z_values.append(Z)
        print(f"p = {p}, Z = {Z}")
    plt.plot(range(40, 330), Z_values, label=f'k = {k_value}')

plt.title("Plot of Z vs. p for different k values")
plt.xlabel("p")
plt.ylabel("Z")
plt.grid(True)
plt.legend()
plt.show()
```

DEPARTMENT OF SOME SUBJECT OR TECHNOLOGY
CHALMERS UNIVERSITY OF TECHNOLOGY
Gothenburg, Sweden
www.chalmers.se

CHALMERS
UNIVERSITY OF TECHNOLOGY